INVESTIGATION OF THE CATALYTIC MECHANISM OF *MYCOPLASMA PNEUMONIAE* L-ALPHA-GLYCEROPHOSPHATE OXIDASE: MUTATION OF THE PROPOSED CATALYTIC BASE

A thesis presented to the faculty of the Graduate School of Western Carolina University in partial fulfillment of the requirements for the degree of Master of Science in Chemistry

By

Craig Matthew Crowley II

Director: Dr. Jamie R. Wallen
Assistant Professor of Chemistry
Department of Chemistry & Physics

Committee Members: Dr. Jack Summers, Chemistry
Dr. Robert Youker, Biology

June 2016

ACKNOWLEDGEMENTS

I would foremost like to thank my research advisor Dr. Jamie Wallen for his constant mentoring and encouragement throughout my time at Western Carolina University. His expertise, patience and understanding added considerably to my graduate experience.

I would like to thank the other members of my committee, Dr. Jack Summers and Dr. Robert Youker for their assistance that they provided at all levels of the research project. Their valuable insight throughout my project was helpful and always welcome.

I'd like to thank Wes Bintz for his help with finding the necessary materials and ordering anything required throughout my research project.

I would also like to thank my family for the support they provided me though my entire life and in particular, I must acknowledge my wife and best friend, Regan, without whose love, encouragement and editing assistance, I would not have finished this thesis.

TABLE OF CONTENTS

LIST OF TABLES

LIST OF FIGURES

LIST OF ABBREVIATIONS

ABTS……2,2'–azino-bis(3–eth-ylbenzothiazoline-6–sulfonic acid)
BPACE…….boric acid, phosphoric acid, citric acid & EDTA
BTZs…….1,3-benzothiazin-4-one
DHAP……dihydroxyacetone phosphate
EDTA……ethylenediaminetetraacetic acid
FAD……..flavin adenine dinucleotide
FMN…….flavin mononucleotide
Glp……glycerophosphate
GlpD…….glycerophosphate dehydrogenase
GlpK…….glycerophosphate kinase
GlpO…….glycerophosphate oxidase
H_2O_2 ……hydrogen peroxide
HRP……..horseradish peroxidase
k_{cat}…….measure of the catalytic production of product under optimum conditions
K_d……..dissociation constant
K_m…….michaelis-menten constant
K_2HPO_4……potassium phosphate monobasic
LB…….lysogeny broth
pKa……..acid dissociation constant
ROS…….reactive oxygen species
[S]…….substrate concentration
SDS-PAGE…….sodium dodecyl sulfate polyacrylamide gel electrophoresis
TYP……..tryptone yeast phosphate media
UV/Vis…….ultraviolet-visible spectroscopy
V……..velocity
V_0…….initial velocity
V_{max}.....maximal velocity

ABSTRACT

INVESTIGATION OF THE CATALYTIC MECHANISM OF *MYCOPLASMA PNEUMONIAE* L-ALPHA-GLYCEROPHOSPHATE OXIDASE: MUTATION OF THE PROPOSED CATALYTIC BASE

Craig Matthew Crowley, M.S. in Chemistry

Western Carolina University (June 2016)

Director: Dr. Jamie R Wallen, Ph.D.

The formation of hydrogen peroxide (H_2O_2) by the enzyme L-alpha-glycerophosphate oxidase (*Mp*GlpO) is essential for the pathogenesis of *Mycoplasma pneumoniae*. *M. pneumoniae* is a pathogen that targets the human respiratory tract, causing at least 40% of all pneumoniae infections, with the most common symptom being tracheobronchitis in children. *Mp*GlpO relays electrons from L-alpha-glycerophosphate to molecular oxygen to form the products dihydroxyacetone phosphate and hydrogen peroxide. Because the formation of hydrogen peroxide is essential for *M. pneumoniae* pathogenesis, the *Mp*GlpO enzyme has emerged as a potential therapeutic target for pneumoniae infections. Recently an X-ray crystal structure of the apo form *Mp*GlpO was determined. Based on features of the proposed active site, a model of glycerophosphate binding was proposed. This study is focused on mutating amino acids that are predicted from the model to bind the glycerophosphate substrate to confirm their role in the catalytic cycle. We were especially interested in investigating the hypothesis that a catalytic base is required for deprotonation of the glycerophosphate substrate, in particular if the histidine residue was essential for catalysis. *Mp*GlpO wild-type and mutants H51A, H51Q, and S348A

proteins were expressed and purified from *E. coli* resulting in 22, 2, 11 and 21 mg of protein respectively from 4.8 liters of Terrific Broth. The activity of the purified enzymes were determined by a ABTS-HRP coupled assay to be 34.7 +/- 4.6 $U*mg^{-1}$, 0.45 +/- 0.18 $U*mg^{-1}$, 2.22 +/- 0.34 $U*mg^{-1}$ and 0.62 +/- 0.22 $U*mg^{-1}$ for wild-type, H51A, H51Q, and S348A respectively. Our results, and the results of our collaborators, indicate that the reaction can still proceed without a catalytic base, but we have identified histidine 51 and serine 348 as having important roles in hydrogen bonding the glycerophosphate substrate in the *Mp*GlpO reaction. Reactivity of the mutants indicates that neither residue acts as the essential base. Future work will focus on understanding the contribution of other residues in the active site that are predicted to bind the substrate.

CHAPTER 1. BACKGROUND

1.1 INTRODUCTION TO FLAVOENZYMES

Oxidation of reduced flavin by molecular oxygen (O_2) is a very important reaction in biochemistry. In vivo, flavins generally exist in the form of flavin mononucleotide (FMN), which is riboflavin phosphorylated at the 5'-OH of the ribityl chain, and flavin adenine dinucleotide (FAD), which is the condensation product of FMN and AMP (Figure 1).[1] Flavins are redox cofactors, capable of receiving up to two electrons from reducing substrates and relaying them to electron acceptors. The flavin coenzymes FMN and FAD catalyze a wide variety of redox and monooxygentation reactions on diverse classes of compounds (Table 1).[2] Both forms of flavin appear to be functionally equivalent, but some enzymes use FMN, others use FAD, and some utilize both.[2] Only about 5-10% of flavoenzymes have a covalently linked FAD, though in most cases these enzymes have a higher redox potential than enzymes that do not.[3] Oxygen is readily available in aerobic organisms and is commonly utilized as an electron acceptor in flavoenzyme catalysis, generating hydrogen peroxide (H_2O_2), which has emerged as an important regulator of signal transduction in eukaryotic organisms.[4]

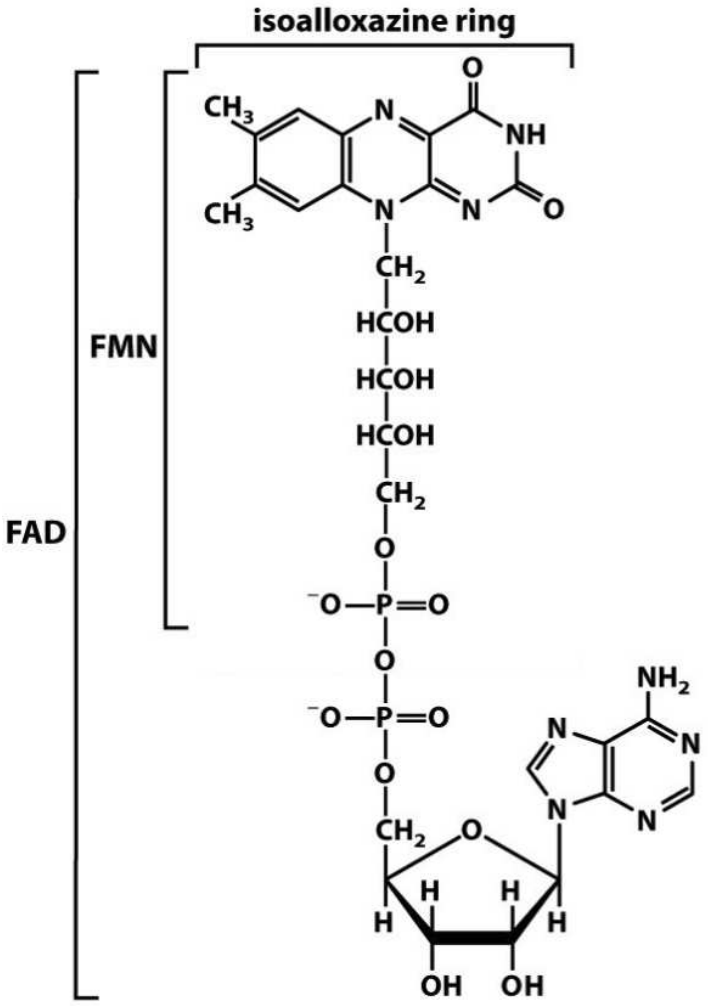

Figure 1: An image of flavin adenine dinucleotide (FAD) and flavin mononucleotide (FMN)

Table 1: Reactions catalyzed by flavin-dependent enzymes[2]

Substrate	Product
	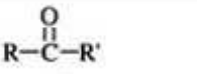
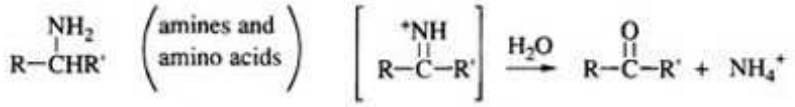	
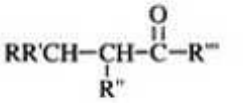	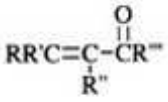
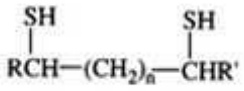	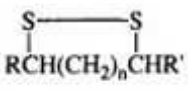
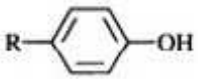	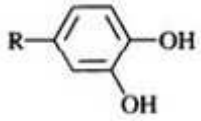
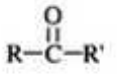	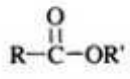
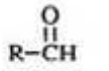	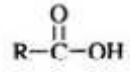
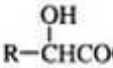	
	

Another reason that the reaction of flavoenymes remains an active area of research is that flavoenzyme oxidases are active generators of reactive oxygen species (ROS). ROS are oxygen containing reactive chemical species that are currently being researched in biochemistry studies because of their involvement in ageing, the process of deteriorating with age, and pathological conditions such as cancer and neurodegeneration.[4] Hydrogen peroxide (H_2O_2), the superoxide anion, and the hydroxyl radical are key members of the class of ROS, which are generated via the respiratory chain cascade but also as byproducts of cellular metabolism[4]. In contrast to the

hydroxyl radical and superoxide anion, the less reactive H_2O_2 is involved in many physiological processes such as mediating immune responses, hypoxic signal transduction, and cell differentiation and proliferation.[5] However, its effects depend on the local concentration, cellular context, and exposure time within the cell (Figure 2).[6] Therefore, H_2O_2 is no longer observed as an unwanted toxic byproduct, but is now considered as having an important role in the control of cellular processes.[5]

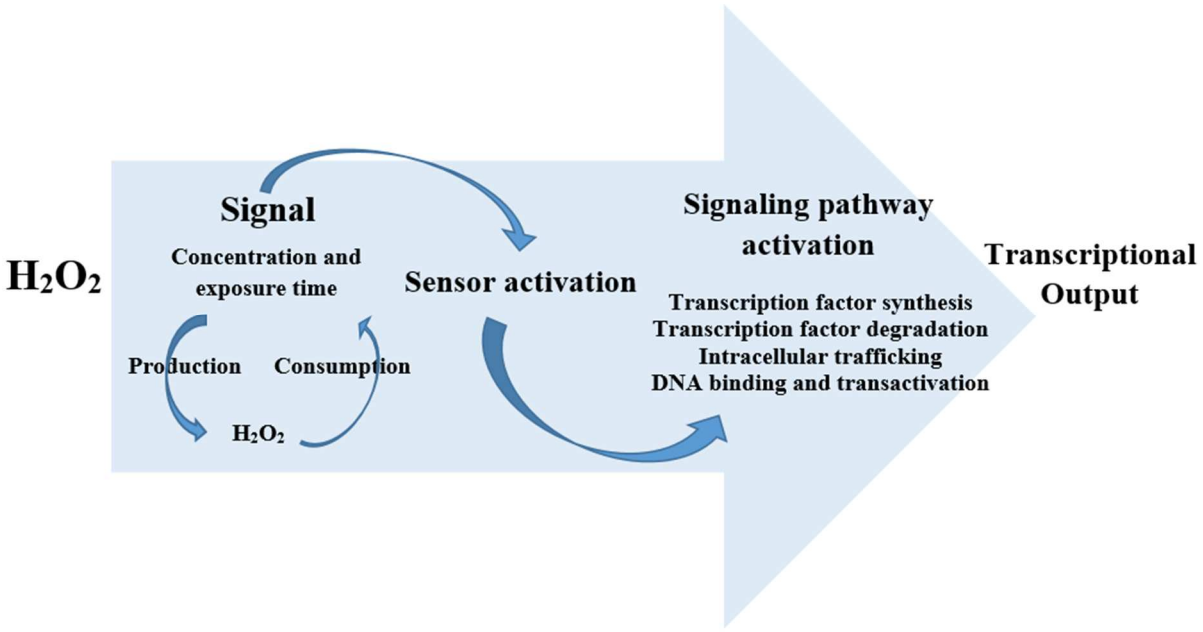

Figure 2: Process of hydrogen peroxide (H_2O_2) signaling pathway activation[6]

Many flavoenzymes are important for cellular redox metabolism and homeostasis, and some flavin-dependent oxidases are well-known drug targets. One example of an FAD-dependent enzyme that regulates metabolism is glycerol-3-phosphate dehydrogenase, which is involved in triglyceride synthesis. An example of a FAD-dependent oxidase used as a drug target is decaprenylphosphroyl-beta-D-ribose, a flavin-dependent enzyme involved in cell wall biosynthesis which has been targeted as a strategy to kill *Mycoplasma tuberculosis*.[4] Inhibition

of this enzyme halts the formation of decaprenylphosphroyl arabinose, a key precursor required for the synthesis of the cell-wall arabinans, thus initiating cell lysis and eventually causing bacterial death.[7] Makarov *et al* synthesized and characterized 1,3-benzothiazin-4-ones (BTZs), a new class of antimycobacterial agents that kill *Mycobacterium tuberculosis in vitro*, *ex vivo*, and in mouse models of tuberculosis.[7]

1.2 L-ALPHA-GLYCEROPHOSPHATE OXIDASES

The FAD-linked oxidation of alpha-glycerophosphate (Glp) to dihydroxyacetone phosphate (DHAP) occurs in at least three different types of enzymes. The first two are alpha-glycerophosphate dehydrogenases (GlpDs) from mitochondria (mitoGlpD[8]) and from bacteria (*bact*GlpD[9]), homologous enzymes having sequences that are approximately 33% identical.[10] The third FAD-dependent Glp-oxidizing enzyme is alpha-glycerophosphate oxidase (GlpO), which is found primarily in heme-deficient lactic acid bacteria such as *Enterococcus casseliflavus* (formerly *Streptococcus faecium*).[11,12] GlpOs are further characterized into type I and type II based on their catalytic mechanisms. Type I and type II GlpO differ in their substrate recognition residues and the distinction between the type I and type II GlpO active sites offers the opportunity to design inhibitors that can selectively block the activity of type II enzymes such as *Mp*GlpO while at the same time not inhibit activity of type I enzymes such of the mitochondrial Glp dehydrogenase of the host.[13] GlpOs are homologous with the bacterial and mitochondrial GlpDs, having sequences approximately 30-43% identical with them but they are distinguished by an insert that is roughly 50 residues long. This insert falls between two segments and interacts with the Glp substrate.[14] A previous study done by Charrier *et al*[15] reported that the GlpO insert represents a flexible region on the protein surface. Enzyme-

monitored turnover analyses of the GlpO without the insert demonstrated a 20-fold increase in the K_m(Glp), indicating that the flexible surface region of the is involved in an important role in mediating efficient flavin reduction by assisting with Glp binding.[15]

Functionally, GlpO differs from GlpD in that GlpO efficiently catalyzes reduction of O_2 to H_2O_2 while GlpD does not, with the *E. casseliflavus* enzyme having a $k_{cat}/K_m(O_2)$ of ~ $10^6 M^{-1}s^{-1}$.[14] Also GlpO is clearly a cytosolic protein while GlpD is membrane bound.[12] A GlpO enzyme is also similar to a GlpD enzyme in that both enzymes will oxidize the glycerophosphate substrate, but an oxidase only uses oxygen as it's electron acceptor while GlpD is able to utilize various compounds as its electron acceptor. The most efficient electron acceptor for *E. coli* GlpD is potassium ferricyanide.[9] GlpO catalyzes the oxidation of L-alpha-glycerophosphate (Glp) at the C2 position to create dihydroxyacetone phosphate as a product. Molecular oxygen (O_2) acts as an electron acceptor during this reaction by receiving two electrons from the flavin of GlpO to generate H_2O_2 (Figure 3). The hydrogen peroxide produced by this reaction is a reactive oxygen species that may be converted to more potent ROS such as peroxide or hydroxyl radicals, and the hydrogen peroxide itself may serve as a cellular signaling molecule.[16] ROS affect cell viability by causing lysis of red blood cells, lipid peroxidation and other oxidative damage.[17]

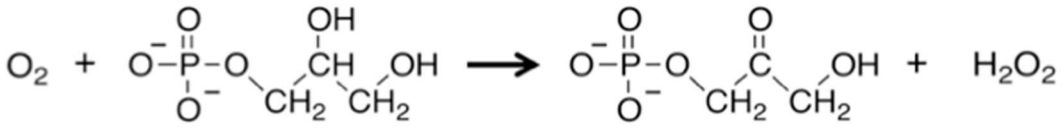

Figure 3: Reaction catalyzed by GlpO

Similarly to their fundamentally different reactivities toward oxygen, flavoprotein oxidases and dehydrogenases also offer a vast contrast in their reactivity with sulfite.[14] All

oxidases stabilize flavin N(5)-sulfite adducts, but no sulfite reaction is observed within the dehydrogenases.[14] It was noted by Parsonage *et al.,* that the reaction sequence leading to the nucleophilic addition of sulfite to the flavin N(5)-position parallels very similarly with the addition of a hydride ion (H^-) to the GlpO flavin (Figure 4).[14] It is possible to use the results obtained from sulfite titrations to determine which residues could be involved in the addition of the hydride ion to the GlpO flavin.

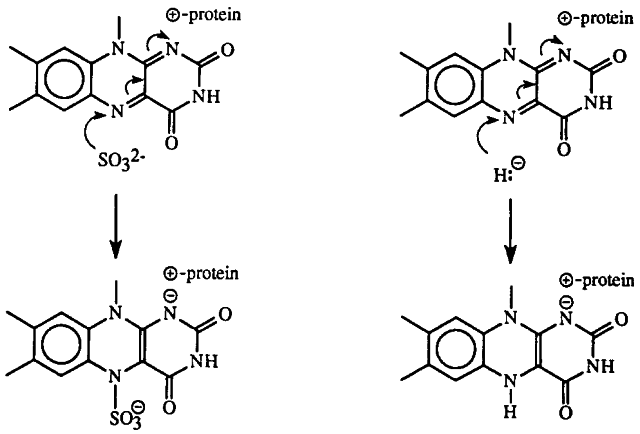

Figure 4: Reaction of GlpO flavin with sulfite and a hydride ion[14]

While all GlpDs are membrane-associated, it is not clear in some cases whether they are integral or peripheral membrane proteins.[10] For example, the mammalian *mito*GlpD has been localized to the outer surface of the inner membrane,[10] but a separate re-study of the enzyme predicts it to be an integral membrane protein with three transmembrane helices.[8] Likewise, *E. coli* GlpD was first reported to require detergent for solubilization during purification, which could lead to the conclusion that it would be an integral membrane protein, but later a His-tagged version of the *E.coli* GlpD was purified without the use of detergent.[10] Another recent study concluded that *E.coli* GlpD was an integral membrane protein with "six transmembrane spanning

regions"[18]. The *Bacillus subtillis* GlpD is found predominantly in the cytosolic fraction following ultracentrifugation of glycerol-grown cell extracts.[19]

Studies of GlpOs from several bacteria have already been accomplished.[10,14] Due to the lack of a GlpO enzyme in mammalian cells the enzyme has become a proposed target for new antibacterial treatment in many organisms. One example of analyzing GlpOs is a native GlpO from *Trypanosoma brucei*, a human parasite that is known for causing African sleeping sickness, was isolated, purified and analyzed to study how to inhibit the enzyme.[20] The study revealed that some potent inhibitors of *T. brucei* GlpO are suramin and alkyl esters of 3,4-dihydroxybenzoic acid.[20] Fairlamb *et al*. discovered that increasing the length of the alkyl substituent resulted in greater inhibition of the GlpO enzyme. They proposed that the inhibitor acts via competition with ubiquinol for the oxidase, with the aromatic regions of the inhibitor forming stable charge-transfer complexes with the alkyl chains of the oxidase that mimic the isoprenoid side chain of ubiquinol.[20] GlpO from lactic acid bacteria such as *Streptococcus* species and *Streptococcus faecium* ATCC 12755 have also been studied[11,12]. Studies on inhibition of the enzyme revealed that *S. faecium* GlpO was inhibited by 25 mM fructose 6-phosphate.[11]

A study of the recombinant GlpO from *Enteroccocus casseliflavus* indicated that the reaction (Scheme 2) obeys a ping-pong (double-displacement) kinetic model, and that the rate-limiting step in the overall reaction is the flavin-reduction.[14] In a ping-pong kinetic model, the enzyme bounces back and forth from an intermediate state (E^*) to its original state. The ping-pong mechanism is characterized by the change into an intermediate form when the first substrate to product reaction occurs. Another key characteristic of the ping-pong mechanism is that one product (P) is formed and released before the second substrate (B) binds (Figure 5).

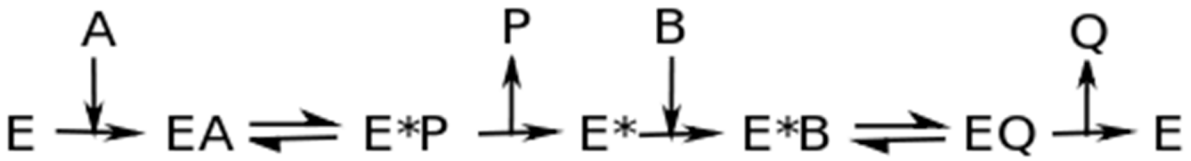

Figure 5: Ping-pong mechanism where the substrate A binds to the enzyme, enzyme-substrate complex EA forms. At this point, the intermediate state, E^* forms. Product (P) is released from E^*, then B binds to E^*, B is converted to Q which is then released as the second product. E^* becomes E, and the process gets repeated. [14]

In contrast, kinetics studies of the *Streptococcus* species wild-type GlpO and a mutant enzyme which had a flexible surface region truncated indicated that the release of DHAP was the rate-limiting step of the enzymatic reaction.[15] This suggests that GlpO enzymes utilize distinct catalytic mechanisms, which leads to the separation between type I and type II GlpOs. Although type I and type II GlpOs are similar in function, they only share less than 20% sequence identity with each other. The visual overlay of the flavin region of *Mp*GlpO, *Ssp*GlpO and *E. coli* GlpD (Figure 6A) and the entire structure overlay of *Mp*GlpO and *S*spGlpO (Figure 6B) shows the divergence between the two groups of enzymes.

A structure-based sequence alignment of these proteins (Figure 6C) provides further details of the comparisons, and is useful for noticing the similarities and differences in the active site residues.[13] Both the type I and type II GlpOs, *S*spGlpO and *Mp*GlpO, have histidine residues in the active site predicted to interact with the glycerophosphate substrate, as well as an absolutely conserved arginine residues predicted to bind the phosphate moiety of the substrate. One of the major differences in the active site residues between the type I GlpO *S*spGlpO and the type II GlpO *Mp*GlpO is the presence of a serine residue in *Mp*GlpO that is not conserved in *S*spGlpO.

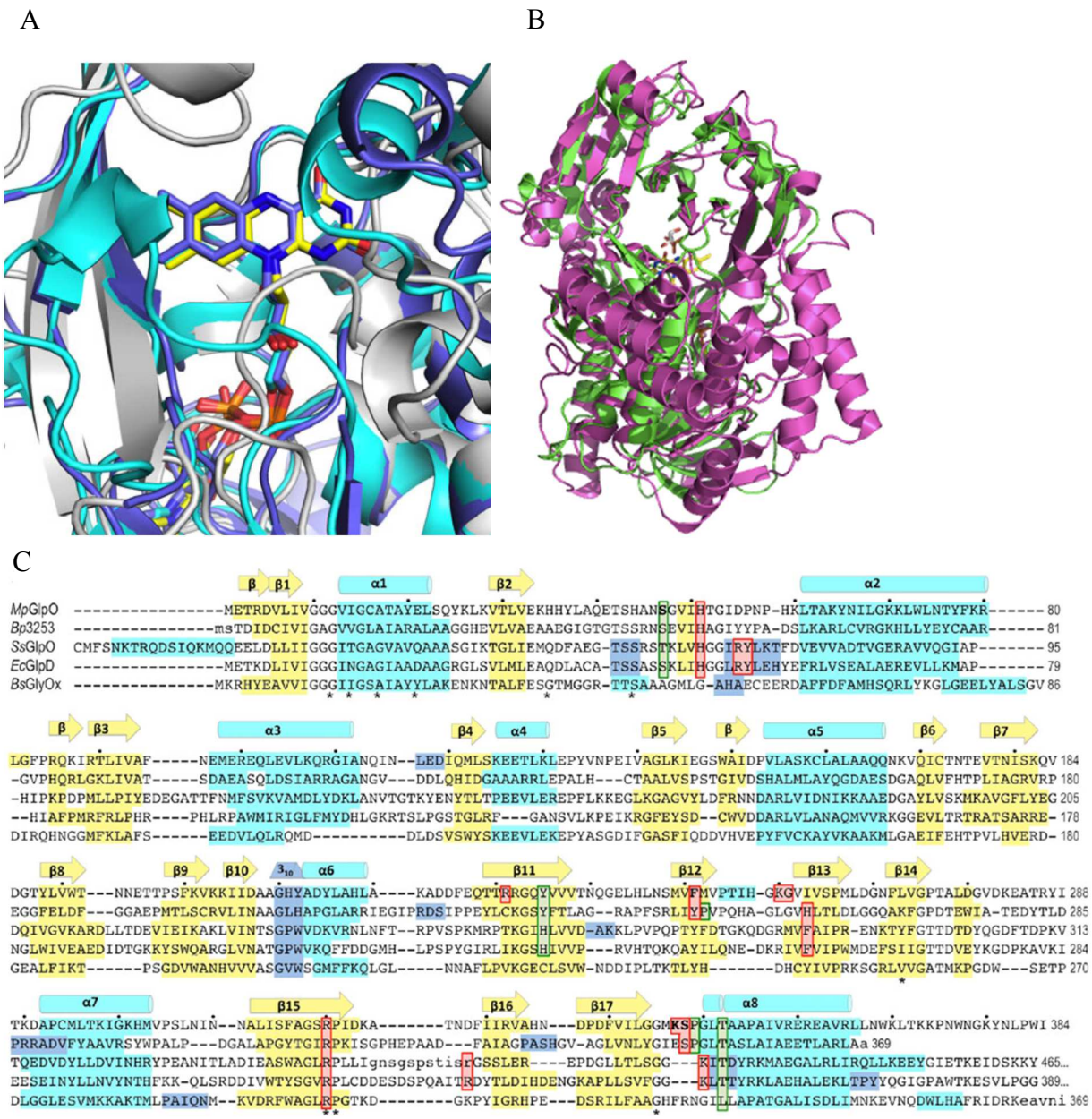

Figure 6: Comparisons of the MpGlpO structure and sequence with select homologs. (A) A flavin region overlay of *Mp*GlpO (off-white protein and yellow FAD) and *Ssp*GlpO (blue; PDB code: 2RGH)[4] and *Ec*GlpD (cyan; PDB code: 2QCU)[9]. (B) Overlay of *Mp*GlpO (green) and *S*spGlpO (magenta) structures. (C) Structure-based sequence alignment of MpGlpO and four enzyme homologs. Conserved residues (*) and residues involved in beta strands (yellow), alpha helices (cyan) and 310-helices (blue) are indicated. Also highlighted are residues noted as being important in substrate binding (red boxes) and flavin binding (green boxes). Dots above the MpGlpO sequence mark every tenth residue and, at the end of each line, a residue number for each of the sequences is shown. Lower case letters are residues that are disordered in the structure.[13]

1.3 *MYCOPLASMA PNEUMONIAE*

M. pneumoniae is a pathogen that is known to target the human respiratory tract, causing at least 40% of all pneumoniae infections, with the most common symptom being tracheobronchitis in children.[21] The *pneumoniae* pathogen infects its host via the mucosal epithelium with the use of a special attachment organelle.[21] This organelle is a polar, negatively charged and elongated cell extension that facilitates motility and cytoadherence to cells from the host.[21] It is composed of a central filament surrounded by an intracytoplasmic space, along with a number of structural and accessory proteins along with adhesins localized at the tip of the organelle.[21] *M. pneumoniae* contains a small genome, lacks a rigid cell wall, and has limited metabolic capabilities.[13] Glycerol metabolism is an important factor in pathogenicity for *M. pneumoniae.*[17,22] The mycoplasmas are missing enzymes necessary for a tricarboxylic acid cycle and an electron transport chain as well as respiratory cytochromes. Since glycerol is an important energy source for this pathogen, enzymes that are involved in glycerol metabolism have become potential drug targets for combating the respiratory infectious disease. In particular, a gene of interest in *M. pneumoniae* is the MPN051, which was annotated as encoding for a glycerol-3-phosphate dehydrogenase (glpD).[13] Despite its annotation as a dehydrogenase, a recent study refers to the encoded protein as a GlpO rather than GlpD due to its use of oxygen in the catalytic reaction and it being a cytosolic protein.[13] MPN051 has been shown to be a constitutively expressed cytosolic FAD-dependent L-alpha-glycerophosphate oxidase.[22] The GlpO gene is tightly linked with the gene that encodes for glycerol kinase (*glp*K) and, together; these enzymes can catalyze the ATP-dependent conversion of glycerol to DHAP.[22] The hydrogen peroxide produced by the *Mp*GlpO enzyme has been shown to be necessary for pathogenicity of the organism, and the ortholog from the animal pathogen, *Mycoplasma*

mycoides subspecies *mycoides* SC, has been shown as a primary virulence factor as well.[11] Also, a study performed by Madhi *et al.* has shown that *Streptococcus pneumoniae* GlpO is responsible for promoting pneumococcal meningitis as well as H_2O_2-mediated cytotoxicity towards human brain microvascular endothelial cells.[23]

In contrast to the behaviors observed with other GlpO enzymes, MpGlpO is able to catalyze the reaction of reduced enzyme with DHAP, which is the reverse of the reaction described in Figure 3. This catalytic property of *Mp*GlpO may represent a control mechanism to prevent excessive generation of H_2O_2, which may be harmful to bacterial cells. The proposed overall catalytic reaction of *Mp*GlpO is shown in Figure 7, with the values for the kinetic parameters seen in the figure illustrated in Table 2. The data in Table 2 indicates that the rate constants of the forward reaction (k_1 and k_3) are much greater than reverse reaction rate constants (k_2 and k_4), indicating the reverse reaction occurs most likely at high concentrations of DHAP.[16]

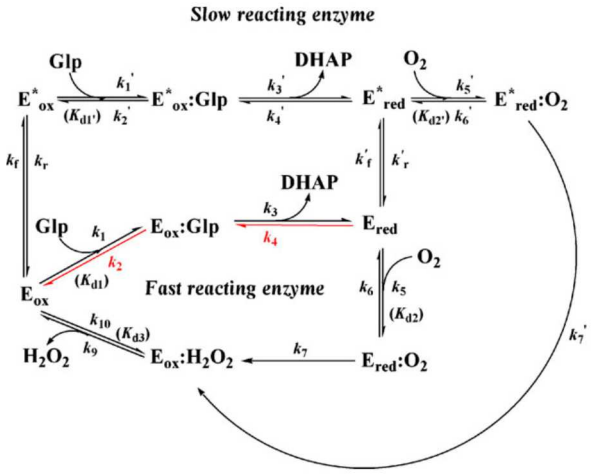

Figure 7: Proposed overall catalytic reaction of *Mp*GlpO. Two enzyme populations (fast- and slow-reacting species) react with substrates in both reactions. The reverse flavin oxidation is indicated by red arrows.[16]

Table 2: Thermodynamic and kinetic parameters for the *Mp*GlpO reaction. ND is not determined[16]

Parameter	Value
Fast-reacting enzyme	
k_1, formation of the E_{ox}:Glp complex ($M^{-1}\cdot s^{-1}$)	83.3
k_2, Glp release (s^{-1})	6 s^{-1}
k_3, enzyme reduction (s^{-1})	199 ± 34
k_4, reverse reaction of E_{red} and DHAP ($M^{-1}\cdot s^{-1}$)	56.5
k_5, k_6, k_{10}	ND
k_7, re-oxidation of reduced enzyme (s^{-1})	627 ± 81
k_9, H_2O_2 release (s^{-1})	4.2 ± 0.1
K_{d1}, dissociation constant for the E_{ox}:Glp complex (mM)	72 ± 18
K_{d2}, dissociation constant for the E_{red}:O_2 complex (mM)	1.3 ± 0.2
K_{d3}, dissociation constant for the E_{red}:H_2O_2 complex (mM)	0.4 ± 0.2
Slow-reacting enzyme	
k_1', k_2', k_4', k_5', k_6'	ND
k_3', enzyme reduction (s^{-1})	2.08 ± 0.01
k_7', re-oxidation of reduced enzyme (s^{-1})	85 ± 11
K_{d1}', dissociation constant of the E^*_{ox}:Glp complex (mM)	1.38 ± 0.02
K_{d2}', dissociation constant of the E^*_{red}:O_2 complex (mM)	0.5 ± 0.1
k_{obs} for inter-conversion of fast- and slow-reacting enzymes (s^{-1})	
$k_f + k_r$	> 6, < 16

A crystal structure of the *Mp*GlpO was recently published (Figure 8) by Elkhal *et al.*[13] The *Mp*GlpO chain is organized into a substrate-binding domain with a core anti-parallel, eight-stranded beta-sheet and a FAD-binding domain with a predominantly parallel, six-stranded beta-sheet (Figure 8).[13] The crystal structure illustrates that the two domains are discontinuous, with the FAD-binding domains including residues 1-87, 149-219 and 330-364, while the substrate-binding domain is formed by residues 86-148 and 227-323.[13]

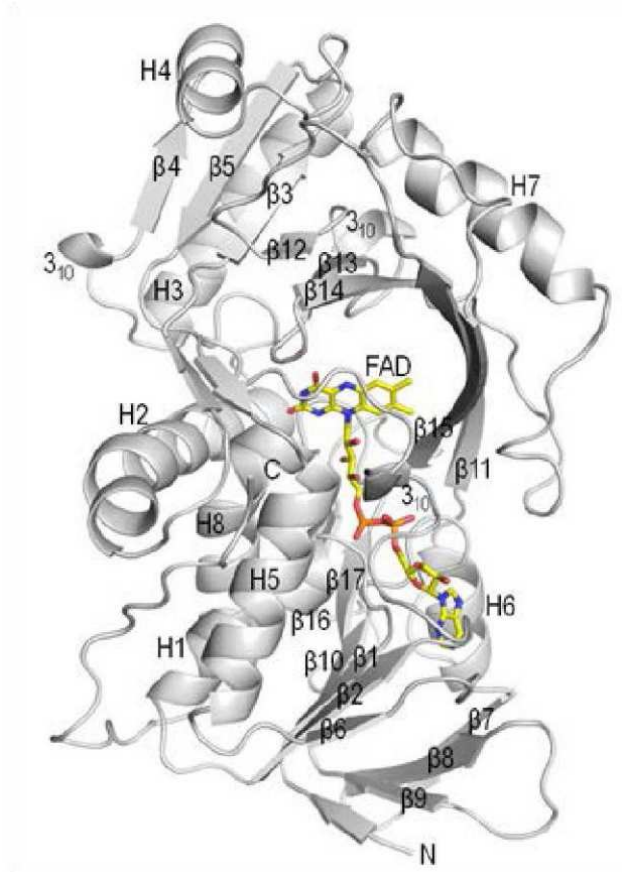

Figure 8: Three-dimensional structure of the MpGlpO determined by x-ray crystallography. The glycerophosphate substrate is predicted to bind near the Flavin adenine dinucleotide (FAD, yellow structure).[13]

A crystal structure of the full-length *Streptococcus* species GlpO (*S*spGlpO) and the truncated wild-type enzyme were solved at 2.4 and 2.3 angstroms respectively. The crystal structure of the type I GlpO indicates that the residues located at the active site of the enzyme most likely to be involved in substrate binding are polar residues such as His65, Arg 346, Lys429, and Arg69[10,13,24]. The positively charged arginine is predicted to interact with the negatively charged phosphoryl group on the glycerophosphate substrate.

The structure shown in Figure 8 is of the apo enzyme without the substrate bound and currently there is no structure data showing how type I (*S*spGlpO) or type II (*Mp*GlpO) enzymes bind to Glp. Two distinct modes were proposed based on the type I and II crystal structures

(Figure 9).[13] We believe that the *Mp*GlpO binding method is a closer representation of the glycerophosphate binding mechanism than the one proposed for *S*spGlpO because the arginine 320 residue, conserved in all 72 close relatives of *Mp*GlpO (Figure 6C), is positioned so that it can contact the phosphate group and the glycerophosphate substrate aligns with the proposed catalytic base, histidine 51, also conserved in all 72 close relatives in *Mp*GlpO (Figure 6C). This predicted binding method positions the C2-hydroxyl of the Glp substrate within close proximity of the flavin cofactor. For SspGlpO it was proposed that the substrate would be oriented the opposite way of Figure 3, with the 3'-phosphoryl moiety near the equivalent of *Mp*GlpO His51 and the C1-hydroxyl interacting with the equivalent of *Mp*GlpO Arg320.[10]

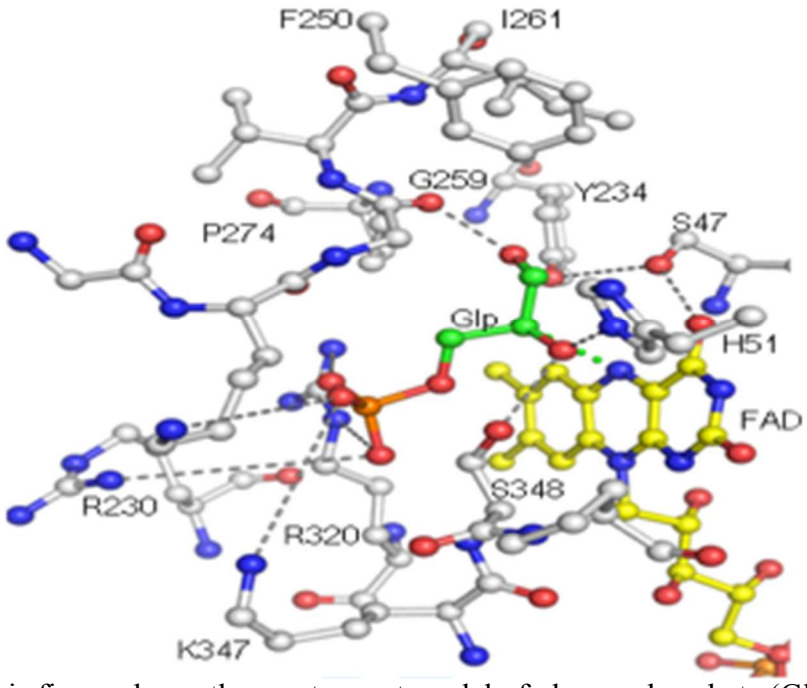

Figure 9: This figure shows the most recent model of glycerophosphate (Glp) binding, with the Glp substrate that has been modeled in shown in green. The amino acids predicted to interact with Glp are shown in white, and a one letter code and number indicate each one. Specific interactions between amino acids in the Glp substrate are indicated with dashed lines. The FAD cofactor is shown in yellow.[13]

Based on the predicted mode of Glp binding to the *Mp*GlpO and the *Ec*GlpD active sites the electron flow during the Glp oxidation proposed to occur according to Figures 10A and 10B.[13] As indicated in Figure 10A (arrows), in *Mp*GlpO, the substrate is in the correct position so that His51 can deprotonate the C2-hydroxyl, promoting the formation of a ketone and helping facilitate the hydride transfer from the C2-atom to the flavin N5-atom. The proposed model of Glp binding also indicates that negatively-charged phosphoryl groups for substrate recognition are important because type I and type II enzymes have three and four positively charged side chains involved in its recognition, respectively (Figure 10).[13]

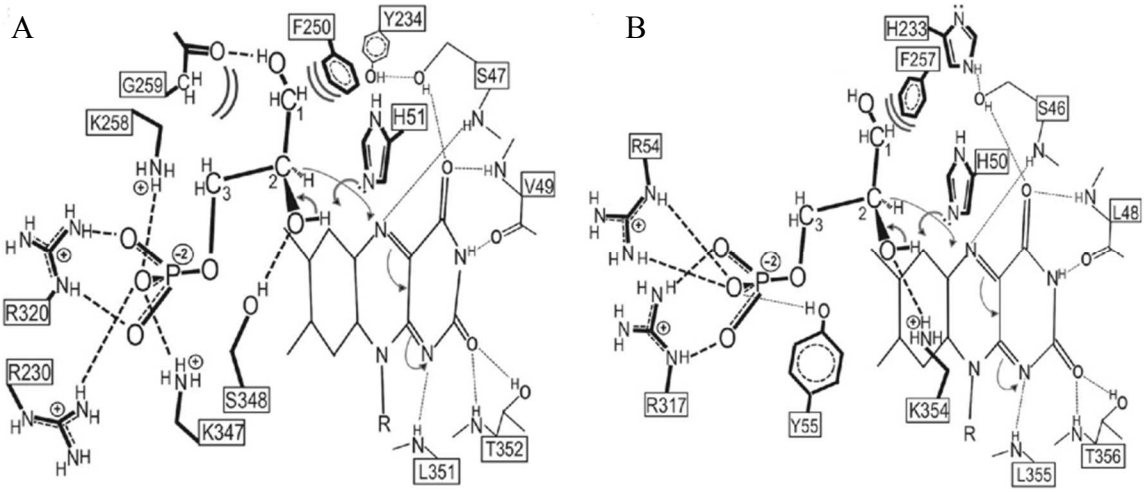

Figure 10: Schematic drawing of residues involved in substrate binding and catalysis in *Mp*GlpO (A) and *Ec*GlpD (B). The *Mp*GlpO active site atoms approximately in the plane of the flavin are shown smaller and with thinner bonds and hydrogen bonds (dashed); atoms in front of the flavin are shown with thicker bonds and hydrogen bonds (dashed). Curved arrows indicate the proposed flow of electrons during the reductive half- reaction. (B) Similar diagram as in (A), showing the *Ec*GlpD active site as a representative of a type I GlpO.[13]

A recent study on the full kinetic reaction of *Mp*GlpO[1] combined with the structural results helps explain some of the differences between type I and type II enzymes.[13] One particular area of interest was the redox potential difference between the *Mp*GlpO flavin, which,

at -167 mV, is much more negative than those seen for type I GlpOs (e.g. *Enterococcus casseliflavus* GlpO at -118 mV).[9,16] Although there are many factors that can influence redox potentials in enzymes, one clear difference in the flavin environment that explains this change in redox potential between the type I and type II enzymes is the fact that the type I GlpO/DH enzymes conserve an active site lysine (equivalent to Lys354 in *Ec*GlpD) (Figure 6C) which has its amino group on the residue at van der Waals distance above the flavin N1/O2 atom. Instead of an active site lysine, the type II enzymes have a conserved neutral serine side chain in that location (equivalent to Ser348 in *Mp*GlpO).[13] An overlay of the *Mp*GlpO active site His51 and Ser348 residues with *S*spGlpO equivalents (Figure 11) shows the difference in the flavin environment. This additional local positive charge in the type I enzymes would make them easier to reduce.[13] As noted in Maenpuen *et al.,* the difference in redox potential is the reason that *Mp*GlpO can catalyze the reverse reaction (DHAP oxidation of the reduced flavin), whereas the type I enzymes tested could not.[16]

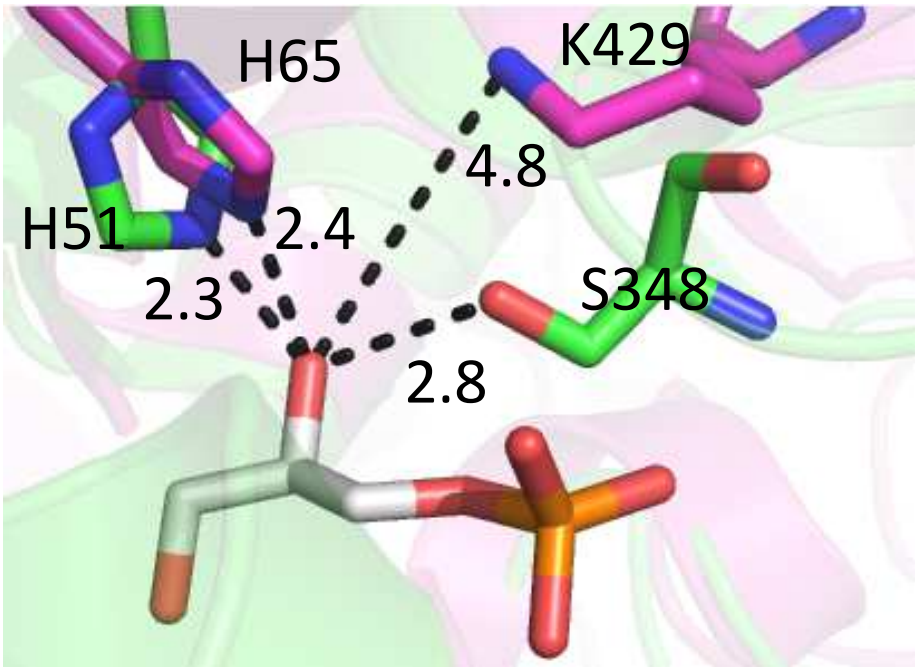

Figure 11: Overlay of the *Streptococcus* species GlpO (magenta) with the *Mp*GlpO crystal structure (green) using PyMol. The glycerophosphate substrate that has been modeled in is shown in white. Dashed lines represent hydrogen bonds between the Glp substrate and the amino acids. The histidine amino acid is conserved in both enzymes, while the Ser348 residue that is present in *Mp*GlpO is not present in *S*spGlpO.

A kinetic analysis of *Mp*GlpO has recently been completed and the steady-state kinetic parameters for *Mp*GlpO were as follows: K_m^{Glp} = 5.5 mM, k_{cat} = 4.2 s^{-1}, and k_{cat}/K_m = 0.76 $mM^{-1}*s^{-1}$ (at pH 7.0 and 4 ºC).[16] This k_{cat} value is four- and nine-fold lower, respectively, than those of GlpO from *Streptococcus sp.* (18 s^{-1})[15] and *E. casseliflavus* (37 s^{-1})[14] at the same temperature (~4 ºC) and pH (~7.0). The K_m value for Glp in the *Mp*GlpO reaction was determined to be 5.5 mM, which is approximately threefold higher and fourfold lower, respectively, than those of *Streptococcus sp.* (2 mM)[10] and *E. casseliflavusi* (24 mM)[14]. The three enzymes have similar K_m values for O_2 (55 uM, 52 uM and 35 uM for *Mp*GlpO, *Streptococcus* sp. and *E. casseliflavius*, respectively).[10,14] Under apparent steady-state conditions (pH 7.0, 25 ºC), the *Mp*GlpO displayed a K_m^{Glp} = 12 +/- 1 mM, k_{cat} = 60.1 s^{-1}, and k_{cat}/K_m = 5 $mM^{-1}*s^{-1}$.[16] These increases in k_{cat} and

k_{cat}/K_m when compared to the steady-state parameters are likely due to the increase in temperature used during the assay.

This thesis presents a continuation of the study of the catalytic mechanism of *Mycoplasma pneumoniae* L-alpha-glycerophosphate oxidase and the effects caused by mutation of the proposed catalytic base His51 as well as Ser348. This study uses a combination of sulfite titrations and standard kinetic assays of wild-type and mutant enzymes to understand the roles of these two amino acids in catalysis. Future work will focus on identifying the importance of other residues predicted to bind Glp from the model in the catalytic cycle as well as comparing the structurally similar type I GlpO (*S*spGlpO) catalytic base equivalent (His65) to the His residue in *Mp*GlpO. Understanding the role of the structurally similar type I SspGlpO could provide some details on the catalytic base in *Mp*GlpO. Further study in this research could provide a solid foundation for guiding further studies of type I GlpOs and mitochondrial Glp dehydrogenases, as well as for continued studies of *M. pneumoniae* glycerol metabolism and the development of novel therapeutics targeting *Mp*GlpO.

CHAPTER 2. INTRODUCTION TO RESEARCH

The purpose of this research is to (1) confirm the role of amino acids in *Mp*GlpO that are predicted to bind the glycerophosphate substrate, (2) identify the base necessary for deprotonation of the glycerophosphate substrate and (3) perform a preliminary study on expression of *S*spGlpO.

The first goal of this study is to test the hypothesis that the amino acids His51, Arg320, Ser348, Phe250, Lys258, Tyr234 and Ser47 bind the glycerophosphate substrate in the *Mp*GlpO enzyme. These amino acids were mutated by site-directed mutagenesis using standard PCR methods. The mutants were then expressed in bacterial cells and purified to compare their activity to that of the wild-type enzyme.

The second goal of this research was to test the hypothesis that His51 is the acid-base catalyst in the *Mp*GlpO reaction by mutating histidine 51 and observing the effect of this mutation on the activity of the enzyme. Mutants of histidine 51 were engineered using standard PCR protocols, bacterial expressions systems, and purified to compare against the activity of the wild-type enzyme.

The third goal of this research was to express *S*spGlpO in order to compare the effects of the catalytic base mutation between type I and type II L-alpha-glycerophosphate oxidases.

CHAPTER 3. EXPERIMENTAL

3.1. MATERIALS

The disodium salt hydrate of FAD, horseradish peroxidase type I (HRP), the diammonium salt of 2,2'–azino-bis(3–eth-ylbenzothiazoline-6–sulfonic acid) (ABTS), and the disodium salt of DL–a–glycerophosphate (Glp) were all purchased from Sigma-Aldrich (St. Louis, MO, USA). Isopropyl-beta-D-thiogalactopyranoside and all antibiotics were purchased from Gold Biotechnology. All of the chromatography columns were purchased from GE Healthcare Biosciences. The plasmids used were a gift from Claiborne lab at Wake Forest University School of Medicine. Oligos used for mutagenesis were purchased from Integrated DNA Technologies (IDT). Restriction enzymes (DpnI) and nucleotides were purchased from New England Biolabs Inc. Herculase Polymerase was obtained from Stratagene.

3.2. METHODS

3.2.1. GENETIC ENGINEERING METHODS

Mutations of the residues of interest were engineered in the gene coding for the wild-type *Mp*GlpO using site-directed mutagenesis and standard PCR methods.[25] Wild-type *Mp*GlpO, which had been cloned into a pET28a vector, was used as the template for the mutagenesis reactions. To confirm that DNA was made during the site-directed mutagenesis reaction, each sample was digested with DpnI to remove wild-type template then ran on a 0.8% agarose gel. The samples that contained DNA were then transformed into DH5 alpha cells to propagate the plasmid and purified using a standard miniprep kit from Qiagen. The plasmid DNA was sequence in-house by Sanger sequencing to confirm the correct mutation. All DNA samples

were sequenced in house using the Big Dye Terminator Kit v1.1 on a ABI 3730xl Sequencer (Applied Biosystem, USA) using an 80 cm capillary array for plasmid DNA or from GeneWiz using T7 and T7 term primers.

3.2.2. EXPRESSION AND PURIFICATION OF HIS_6-*Mp*GlpO

A streak of colonies of *E. coli* BL21 harboring the His_6-*Mp*GlpO expression plasmid, pET28a-*mpglpo*, was inoculated into 100 mL Terrific Broth [1.2%(w/v) peptone, 2.4%(w/v) yeast extract, 0.4%(v/v) glycerol, 15.6 mM KH_2PO_4, and 72 mM K_2HPO_4] (in a 500 mL Erlenmeyer flask) containing 50 micrograms/mL kanamycin, and placed in a shaking incubator at 37 ^oC until the optical density reached 1.0. All colonies should have the same plasmid, but some cells might express better than others, so taking a selection of colonies improves the odds of picking a good one. The culture was then inoculated into 5 x 800 mL Terrific broth containing 50 micrograms/mL kanamycin once the flask reached an optical density of ~1.0. The large-scale cultures were grown at 37 ^oC until the absorbance at 600 nm reached 0.6-0.9. The cultures were then cooled to 25 ^oC and were induced by addition of isopropyl-beta-D-thiogalactopyranoside (IPTG) at a final concentration of 1 mM, and grown overnight at this temperature for approximately 16 hours. Cells were harvested by centrifugation at 3500 g for 30 minutes at 4 ^oC and stored at -80 ^oC until use.

Harvested cells were resuspended in 50 mM sodium phosphate, pH 7.0, containing 200 mM NaCl, 10% v/v glycerol and 10 mM imidazole. Cells were lysed by ultrasonication using a Branson 250 Sonifier using seven 1-minute pulses with an output of 5 and the duty cycle set to constant. The lysed cells were then centrifuged at 35,000 g for one hour and then the supernatant is removed, and the cells centrifuged with another high-speed spin (35,000 g) for 30 minutes

before being loaded onto a 5 mL Ni-NTA column pre-equilibrated with 50 mL of 50 mM sodium phosphate buffer, pH 7.0, containing 200 mM NaCl, 10% v/v glycerol and 10 mM imidazole. *Mp*GlpO protein was eluted with 500 mM imidazole after washing the column with 50 mL 20 mM imidazole. The pooled yellow fractions were loaded onto a 5 mL SP-Sepharose HP column equilibrated in 50 mM potassium phosphate, pH 7.0, 0.5 mM EDTA and 100 mM NaCl. The column was washed with 50 mM potassium phosphate, pH 7.0, 0.5 mM EDTA and 100 mM NaCl before *Mp*GlpO was eluted with a 100 mM to 1 M NaCl gradient over 200 mLs. Fractions were analyzed by SDS/PAGE, the fractions containing the correctly sized protein band were then pooled, and concentrated using an Amicron Ultra-15 Centrifugal Filter. A solution of 1 mL of purified enzyme was exchanged into 50 mM potassium phosphate, pH 7.0, and 0.5 mM EDTA using a HiPrep 26/60 Sephacryl S-200 HR column. The enzyme was then concentrated to less than 1 mL and placed into 10 microliter aliquots in microcentrifuge tubes, and kept at -80 ^{o}C until use. The protein amount was determined using a NanoDrop 2000 Spectrophotometer based on the FAD molar extinction coefficient of 12.4 $mM^{-1}cm^{-1}$ at 450 nm.

3.2.3. ENZYME ASSAY

The activity of His_6-*Mp*GlpO was measured by monitoring the amount of H_2O_2 formed using the 2-2'-azino-bis(3-ethylbenzothiazoline-6-sulfonic acid)/horseradish peroxidase (ABTS-HRP) assay system (Figure 12).[16]

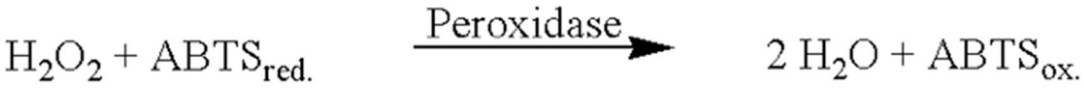

Figure 12: Schematic of how horseradish peroxidase uses the H_2O_2 generated from the *Mp*GlpO-catalyzed reaction to oxidize reduced ABTS to generate oxidized ABTS, which is dark green with a lambda max at 420 nm and a molar absorption coefficient of 42.3 $mM^{-1}cm^{-1}$ (per mole Glp consumed).[16]

HRP uses the H_2O_2 generated from the His_6-*Mp*-GlpO-catalyzed reaction to oxidize reduced ABTS to produce oxidized ABTS, which has a dark green color with a lambda max at 420 nm and a molar absorption coefficient of 42.3 $mM^{-1}*cm^{-1}$.[26] The standard assay solution in 50 mM sodium phosphate buffer (oxygen concentration of approximately 0.26mM), pH 7.0, typically contained 100 mM Glp, 1 mM ABTS and 600 nM HRP at 25 ^oC. The buffer was saturated with oxygen by stirring the buffer with a magnetic stir-bar at high speeds overnight. The activity of the enzyme was measured by monitoring the increase in absorbance at 420 nm due to the oxidation of ABTS. One unit of His_6-*Mp*GlpO activity was defined as the amount of enzyme required to oxidize 1 micromole of Glp per minute. Specific activity of the enzyme was calculated by multiplying the rate of the reaction by the volume of the reaction and then dividing by the mass of the total protein to give units of micromole$*min^{-1}*mg^{-1}$.

3.2.4 STEADY-STATE KINETICS

Apparent steady-state kinetics analysis of the *Mp*GlpO reaction was performed in air-saturated 50 mM sodium phosphate buffer (saturated oxygen concentration is approximately 0.26 mM), pH 7.0, at 25 ^oC at various concentrations of D,L-glycerophosphate (0.1 mM – 51.2 mM) using the ABTS-HRP assay. The reactions were monitored at 420 nm as described above. The reactions follow apparent steady-state kinetics because the concentrations of one substrate were

changed (Glp) while the other substrate (O_2) stays at the same concentration. Under these conditions, the enzyme behaves just like a single-substrate enzyme and gives apparent K_m and V_{max}. The initial rates were calculated using the first five seconds of the reaction and then plotted versus Glp concentration. The initial rate at this time should represent the maximal rate of the enzyme. Apparent kinetic parameters were calculated a Hanes-Woolf plot, where [S] is substrate concentration, V is initial velocity, K_m is the binding affinity of enzyme for substrate and V_{max} is the maximal velocity of the reactions.

$$\frac{[S]}{V} = \left(\frac{1}{Vmax}\right) * [S] + \frac{Km}{Vmax}$$

3.2.5. SULFITE TITRATION ASSAY

Many flavoprotein oxidases react with sulfite to form a reversible adduct at the flavin N5-position.[27] The reaction of sulfite with *Mp*GlpO was measured at 450 nm; 35.4 micromolar enzyme (final concentration) was treated with sulfite in 0.8 mL of 50 mM potassium phosphate, 500 mM EDTA, pH 7.0, under aerobic conditions at 25 ºC. Oxidized flavins show a high absorbance at 450 nm,[27] as the flavin forms the sulfite-adduct the flavin is no longer oxidized and the 450 nm absorbance decreases. The enzyme and buffer was titrated with a 1 M sodium phosphate solution, using 5-minute incubation periods, to get final sulfite concentrations of 0 to 50 mM. The dissociation constant for substrate binding (K_d) was determined by plotting the Abs_{450} versus sulfite concentration. If the rate-determining enzymatic step (k_2) is slow compared to substrate dissociation ($k_{-1} >> k_2$), the Michaelis constant K_m is roughly the dissociation constant K_d of the enzyme-substrate complex.[28]

$$E + S \underset{k_{-1}}{\overset{k_1}{\rightleftharpoons}} ES \xrightarrow{k_2} E + P$$

3.2.6. PH TITRATION USING MULTI-BUFFER SYSTEMS

In order to determine the pKa of the important catalytic residues in the active site of *Mp*GlpO wild-type we used a pH titration following the standard assay conditions. Attempts at a pH titration of wild-type *Mp*GlpO enzyme were used with a variety of multi-buffer systems. Using a multi-buffer system, buffers may be prepared at a desired pH value without altering the chemical composition of the buffered component. In order to analyze the pH-dependent properties of *Mp*GlpO multi-buffer systems, or universal buffers, known as the Britton-Robinson buffer (effective from pH 2.6 to 12), BPACE buffer, and a modified universal buffer were utilized.[29] The Britton-Robinson buffer system contains three different buffering components: 40 mM citric acid (pK_a = 3.0, 4.6 & 5.8), 40 mM phosphate (pK_a = 6.9 & 11.6), and 40 mM boric acid (pK_a = 9.2).[29] The pH of the Britton-Robinson buffer was adjusted using 0.2 M NaoH. BPACE buffer consists of 10 mM sodium phosphate, 10 mM boric acid, 10 mM sodium citrate and 1 mM EDTA at pH 7.0. [30] The pH of the BPACE buffer was adjusted with either ammonium hydroxide or 20% sulfuric acid. The modified universal buffer consisted of boric acid, citric acid, maleic acid, Trizma base and sodium hydroxide. The pH of the modified universal buffer was adjusted using 1.0 M HCl or 1.0 M NaOH. Each of the mixtures were aliquoted into 10 tubes with 5 mL volume. The aliquots were separately mixed with the corresponding pH adjusting solutions and the pH values of the resulting solutions were measured at room temperature using pH paper. The pH paper was used because it was easier to test the small volumes of the buffer solutions using pH paper instead of a pH probe. The aliquots were oxygenated overnight and then the pHs of the solutions were tested again to determine if they were stable the next morning. If the pH of the solutions remained the same, 100 mM Glp, 1 mM ABTS and 600 nM HRP was added to each aliquot. The activity of the *Mp*GlpO wild-type

enzyme was analyzed from pH 3 to pH 10 by monitoring the increase in absorbance at 420 nm using the ABTS-HRP assay.

3.2.7 EXPRESSION OF *S*SPGLPO

Purification of the type I *Streptococcus* sp. GlpO wild type enzyme and the two catalytic base mutants H65Q & H65A will provide details on the function of the active-site His in type I vs type II GlpOs. Understanding the role of the catalytic base in type I GlpOs such as *Streptococcus* sp. could also be useful in guiding further studies of other type I and type II GlpO/DH enzymes. Test expressions of *S*spGlpO wild-type and mutant protein were performed using a wide variety of bacterial cell lines and media following established protocols. The media contained 10 ug/mL tetracycline, 100 ug/mL ampicillin, and 30 mM glucose. Growth of the media was at 37 ^{o}C until the optical density of the cells reached 1.0 and were then cooled in an ice bath before induction with 0.5 mM IPTG. The cultures were kept at 23 ^{o}C for 7-10 hours before harvesting. Wild-type protein expression was tested using XL1-Blue, B834/pREP4, HMS174, and BL21 bacterial cell lines. Each of the cell lines were tested in LB, TYP, Terrific Broth, and auto-induction media in order to get expression of the correct protein band at approximately 65,000 Daltons. Expression of the desired protein was analyzed using SDS-PAGE gels.

CHAPTER 4. RESULTS AND DISCUSSION

4.1. EXPRESSION AND PURIFICATION OF HIS_6-MPGLPO

Recombinant wild-type *Mp*GlpO, proposed catalytic base mutants H51Q and H51A, as well as mutant S348A were all expressed as soluble enzymes in *E. coli* BL21 cells cultured in Terrific broth and induced using IPTG at 25 ^{o}C. *Mp*GlpO wild type and mutants were purified using Ni-NTA affinity chromatography, SP-Sepharose cation exchange chromatography, and size exclusion gel chromatography as described in the Experimental section. This protocol resulted in approximately 22, 11, 3, and 21 mg of purified enzyme for *Mp*GlpO wild-type, *Mp*GlpO H51Q, *Mp*GlpO H51A, and *Mp*GlpO S348A, respectively. The size exclusion column helps determine if the protein elutes at the right size and that no aggregation is occurring, and with our enzyme eluting at the proper time as estimated by the column standards (Figure 13), we assume that the protein eluted as a monomer and is correctly folded (Figure 14). The lambda max of the peak (*Mp*GlpO ~ 47,348.62 daltons) shown in Figure 14 eluted at approximately 140 mLs. The standard in Figure 13 that eluted at 145 mLs had a molecular weight of 44,000 daltons, therefore concluding that the *Mp*GlpO wild-type protein eluted at the correct time should be properly folded. There is a slight shoulder present in the chromatograph of wild-type enzyme, perhaps illustrating the formation of some dimers or other oligomers. The purified enzyme exhibited spectral characteristics that are typical of a FAD-bound enzyme, with a maximum absorbance located at 448 nm and a 280:450 ratio of 6.5, which is consistent with other flavoenzymes (compared to 7.0 for the enzyme from *E. casselifalvus).*[14]

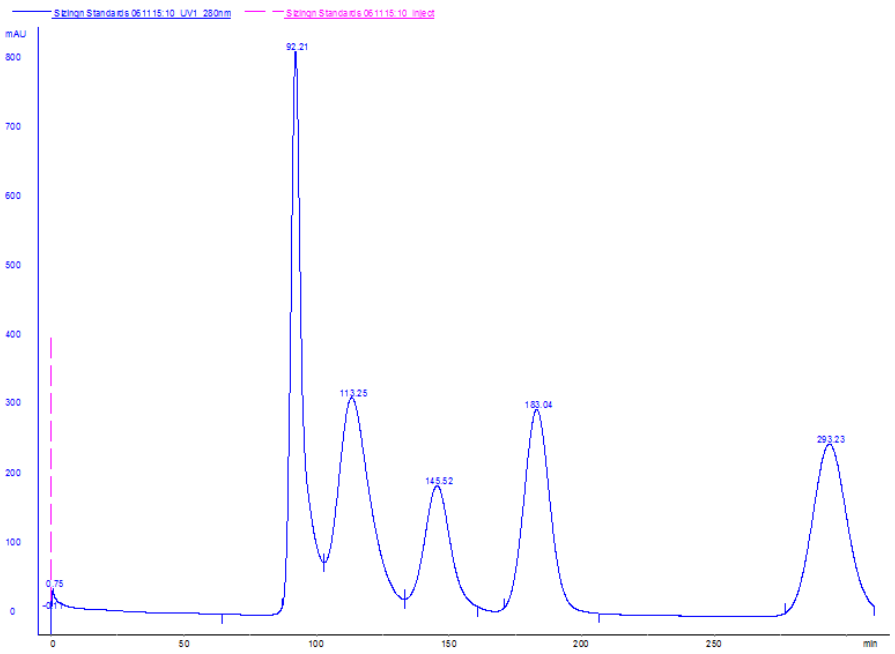

Figure 13: Standards of the size-exclusion column. The molecular weights of the standards used are 670 kDa, 158 kDa, 44 kDa, 17 kDa and 1.3 kDa and they eluted at 92, 113, 145, 183, and 293 minutes, respectively.

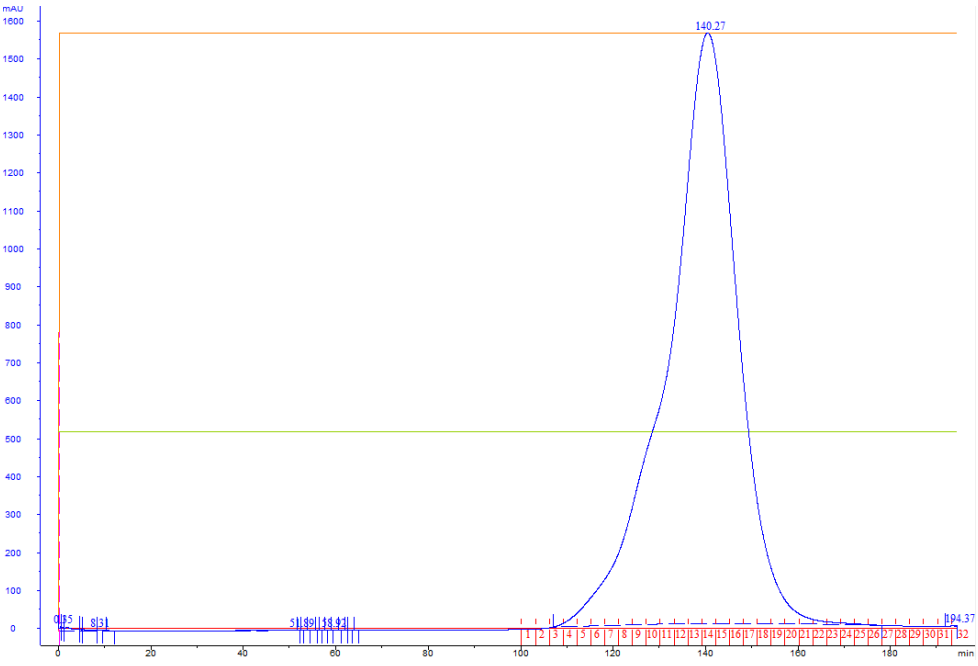

Figure 14: This figure illustrates the chromatogram taken during the gel filtration column of *Mp*GlpO wild-type. The lambda max of the peak (*Mp*GlpO ~ 47,348.62 daltons) shown eluted at approximately 140 minutes. Because the enzyme is not elongated, we are able to use the

standards of the sizing column to estimate if the protein is aggregating together or if it eluting as a monomer. Because the column standard at 44,000 daltons elutes at approximately 145 minutes it makes sense that *Mp*GlpO elutes at about the same time if not a little faster.

In order to ascertain that there were no dramatic structural changes caused by the His51 and Ser348 mutations, the sizing column chromatogram of each enzyme was analyzed as it was being purified to see if it had the correct elution profile. The H51Q, H51A (Figure 15), and S348A (Figure 16) proteins all eluted at approximately 135-141 minutes, concluding that the mutations had no substantial effects on *Mp*GlpO folding.

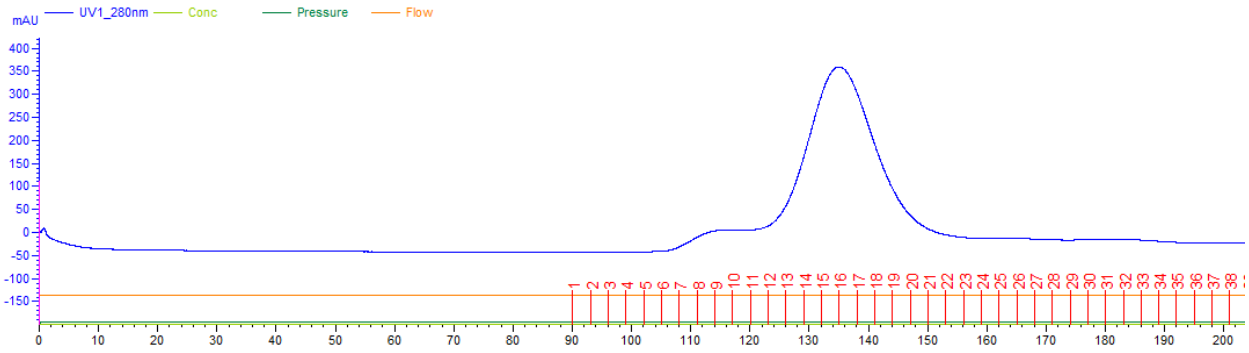

Figure 15: Chromatogram of mutant H51A of the gel filtration column. The lambda max of the peak shown eluted at approximately 136 minutes.

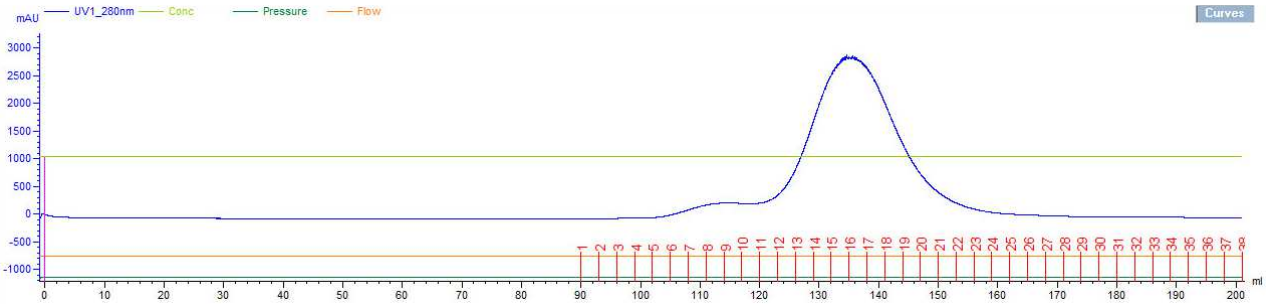

Figure 16: Chromatogram of mutant S348A of the gel filtration column. The lambda max of the peak shown eluted at approximately 135 minutes.

4.2. ENZYME ASSAY

The standard kinetic assay was performed in 50 mM sodium phosphate buffer, saturated oxygen substrate (approximately 0.26 mM), pH 7.0, at 25 ^{o}C typically containing 200 mM D-L-Glp, 1 mM ABTS, and 600 nM HRP. Specific activities of the enzymes were determined by multiplying the rate of the reaction by the volume of the reaction and then dividing by the mass of the total protein to give units of micromole*min^{-1}*mg^{-1}. Using the ABTS-HRP coupled assay to monitor the increase of absorbance at 420 nm due to the oxidation of ABTS, the absorbance values were plotted against time (in seconds) in order to determine the initial velocity of the enzyme (Figure 17). The initial velocity provides a rate for the enzyme prior to substantial substrate depletion and product accumulation. The initial velocity is determined from the slope of the curve at the beginning of the reaction, when the reverse reaction is insignificant.[16] The initial velocity of the reaction was divided by the molar absorption coefficient of ABTS (42.3 mM^{-1}*cm^{-1}) in order to calculate the rate of the reaction in units of mM ABTS*min^{-1}. The specific activities of the wild-type enzyme, H51Q, H51A, and S348A mutants were determined to be 34.7 +/- 4.6 U*mg^{-1}, 2.22 +/- 0.34 U*mg^{-1}, 0.45 +/- 0.18 U*mg^{-1}, and 0.62 +/- 0.22 U*mg^{-1} respectively.

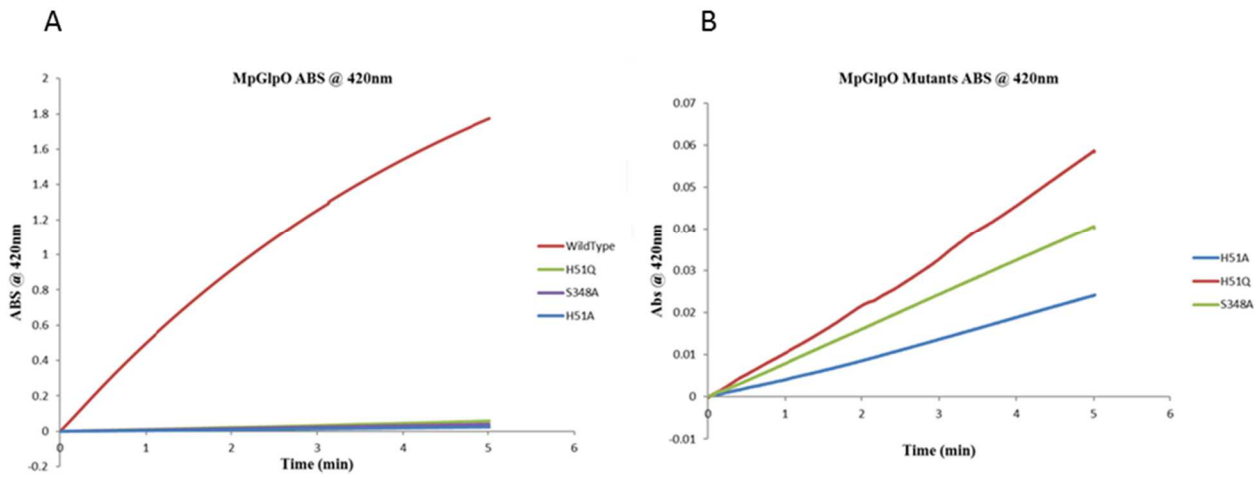

Figure 17: (A) Standard kinetic assay for wild-type, H51A, H51Q & S348A *Mp*GlpOs monitored at 25 ºC . The assay reactions were monitored by the ABTS-HRP assay using a Cary UV/VIS spectrophotometer. The standard assay solution in oxygen-saturated 50 mM sodium phosphate buffer (pH 7.0) typically contained 100 mM Glp, 1 mM ABTS and 600 nM HRP at 25 ºC. The activity of the enzyme was measured by monitoring the increase in absorbance at 420 nm due to the oxidation of ABTS (B) Re-plot of A to more easily see rate of *Mp*GlpO mutants. Our results show severely compromised activity when His51 or Ser348 is altered.

Every time that one of the mutants' specific activity was tested using the ABTS-HRP assay, *Mp*GlpO wild-type was tested alongside it in order to make sure that the assay was working correctly each time. Reactions of mutant and wild-type enzyme were tested in triplicate on one day and then repeated in triplicates on a separate day in order to verify the results. The average of the slopes from the reactions were used in calculating the specific activity of the *Mp*GlpO enzyme.

Mutation of either the His51 or Ser348 residue severely compromised enzyme activity. The H51Q mutation was 6.5% as active as wild-type, while H51A was approximately 1.3% as active as wild-type. It is also important to note that the activity of H51Q was higher than H51A in Figure 17B. Through site-directed mutagenesis, the active-site histidine was replaced with alanine in order to assess the contribution of the side chain in forming hydrogen bonds with the glycerophosphate substrate. Based on our data it would lead us to believe that the polar side

chains of amino acids histidine and glutamine, that are absent in alanine, are important for hydrogen bonding with the substrate. However, if His51 were the true catalytic base, any mutation would result in the enzyme having less than 1% of wild-type activity remaining, which leads us to believe His51 may be more important for substrate recognition than as a catalytic base. Our results illustrate that the reaction can still proceed without a catalytic base, with the H51Q mutation retaining 6.5% of wild-type activity. Recent studies have shown that naturally occurring flavins can act as stand-alone catalysts in aqueous buffer.[31] The study compared the catalytic activity of FMN alone with that of NRPS oxidase EpoB-OX. Under matching conditions, kinetic parameters for FMN and EpoB-OX were determined resulting with similar K_m values of 1.1 +/- 0.1 mM and 2.1 +/- 0.4 mM for FMN and EpoB-OX respectively.[31] However the rate constant for FMN (k_{cat} = 0.47 +/- 0.04 min^{-1}) was an order of magnitude lower than that for EpoB-OX (k_{cat} = 7.7 +/- 0.8 min^{-1}).[31] This evidence suggests that the oxidase may contain a base in the active site that causes greater catalytic efficacy when compared to FMN alone, however the reaction is still able to proceed solely with the flavin. It is likely that EpoB-OX enzyme is able to bind both the flavin and the substrate within close proximity, helping to facilitate the reaction, while the reactions catalyzed by the FMN by itself require productive collisions of the flavin with the substrate in solution. A possible residue that could be assisting the His51 mutants in forming hydrogen bonds with the substrate is Ser348, which is conserved in all 72 *Mp*GlpO relatives.[13] Ser348 is within the distance needed for hydrogen bond contacts of the modeled Glp substrate C2-hydroxyl as seen in Figure 11. The serine hydroxyl group is able to form hydrogen bonds with a variety of polar substrates,[32] which could allow them to assist the His51 mutants in recognizing the proper substrate. Mutation of the Ser348 mutant to alanine also resulted in approximately 2% of wild-type activity, concluding that the hydroxyl group on

serine, and any hydrogen bonds that would be formed, are important for substrate recognition and catalysis.

4.3. STEADY-STATE KINETICS

Apparent steady state kinetics of *Mp*GlpO wild type using saturated oxygen and Glp as substrates were investigated at 25 ^{o}C, pH 7.0, using the 2,2'-azino-bis(3-ethylbenzothiazoline-6-sulfonic acid)/horseradish peroxidase (ABTS/HRP) assay as described in the Experimental section. Initial rates at various concentrations of glycerophosphate were measured. Kinetic parameters of the enzyme reaction obtained from a direct Michaelis-Menten or Hanes-Woolf plot (Figure 18) were K_m^{Glp} = 14 +/- 2.3 mM, K_{cat} = 75 +/- 3.6 s^{-1}, resulting in a specificity constant of 5.3 $mM^{-1}*s^{-1}$. This specificity constant is similar to the previously reported K_{cat}/K_m of 5 $mM^{-1}s^{-1}$ by Maenpuen *et al*.

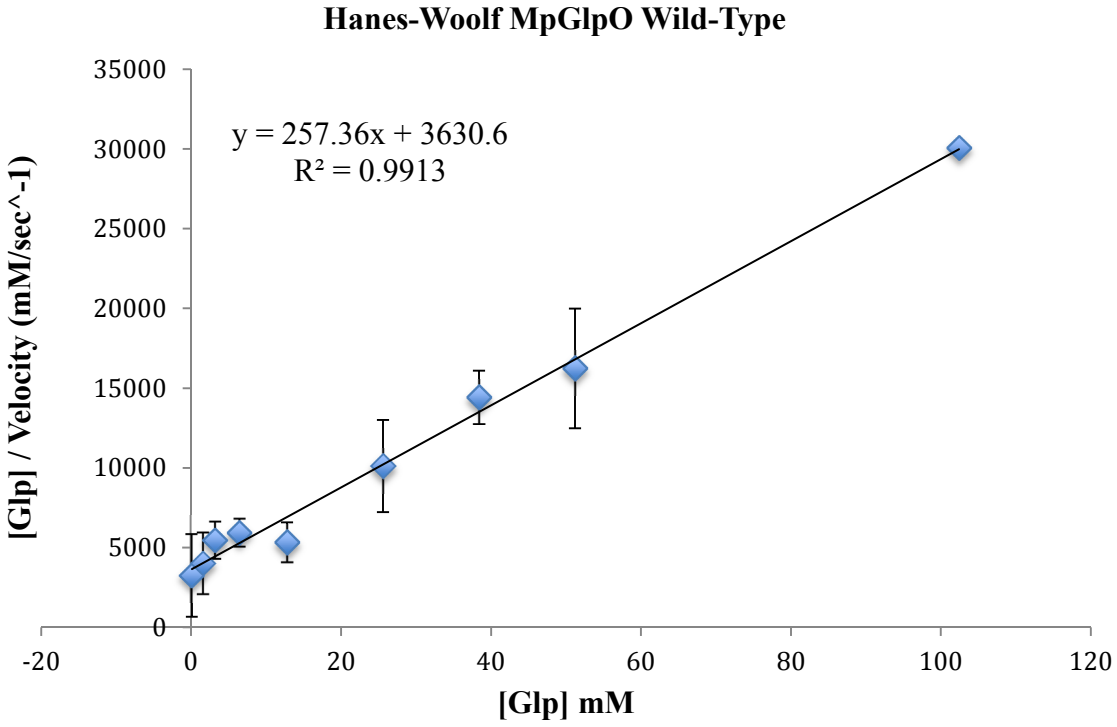

Figure 18: Apparent steady-state kinetic parameters of wild-type MpGlpO at 25 ºC. Initial rates obtained from various concentrations of Glp (0.1 mM – 102.4 mM) were measured, and plotted using [Glp]/V_o versus [Glp]. Kinetic parameters were determined using the equation $[S]/V=(1/V_{max}*[S])+K_m/V_{max}$.

The k_{cat} of 75 s^{-1} seems to be on par with other oxidases, comparable to that seen for GlpOs from *E. casseliflavus*[14] and *Streptococcus* sp.[15] which gave k_{cat} values of 70-90 s^{-1} at 25 ºC. Due to the low specific activity of the mutants during the standard assay that uses 200 mM Glp, full kinetic traces of the mutants were attempted but produced no reliable data. Steady-state kinetics of the H51Q mutant were performed at enzyme concentrations of 5.16 nM, 51.6 nM, 103.2 nM, 206.4 nM, 412.8 nM and 825.6 nM using a range of 100 mM to 500 mM Glp substrate. Unfortunately, we were still unable to determine a Vmax at these high enzyme concentrations, indicating that the rate of the reaction is too low or that the Km of the mutant is too high in order to obtain a full kinetic trace.

4.4. SULFITE TITRATION ASSAY

Many flavoprotein oxidases are characterized by their ability to react with sulfite and form a reversible adduct at the flavin N5-position.[27] The flavin-sulfite adduct is stabilized by interactions with many residues at the active site as indicated by a structural study of flavocytochrome b_2 complexed with sulfite, including the active-site histidine and serine residues.[33] Type I GlpOs including *Ecass*GlpO and *Ssp*GlpO give similar values of K_d = 0.82 mM and 1.5 mM[14,15] and in both enzymes the flavin becomes fully reduced with sulfite. In this study, we performed titrations using a similar protocol with freshly prepared *Mp*GlpO. For wild-type *Mp*GlpO, our titrations with sulfite provided a K_d = 3.3 mM, which is similar to the 3.0 mM K_d that was determined by a previous study.[13] Additionally, *Mp*GlpO showed that its flavin absorption was only bleached by about 50%, through the addition of sulfite (Figure 19), which also agrees with the sulfite titrations previously reported on *Mp*GlpO.[13] As of this moment we do not have a clear idea as to why only half of the enzyme reacts with sulfite. We can speculate that perhaps the inactive species is the result of nonproductive site architecture (nonproductive for FAD binding or sulfite adduct formation). Another possibility could be that some oligomerization is occurring, as seen in the very slight shoulder present in the size exclusion chromatograph (Figure 14), and the species of *Mp*GlpO that is forming dimers are unable to bind with sulfite. None of the other GlpO enzymes previously described show this behavior in sulfite titrations. Unfortunately, a sulfite titration with H51A mutant was unable to be performed due to low protein yield from purification and will need to be done for future work in this area.

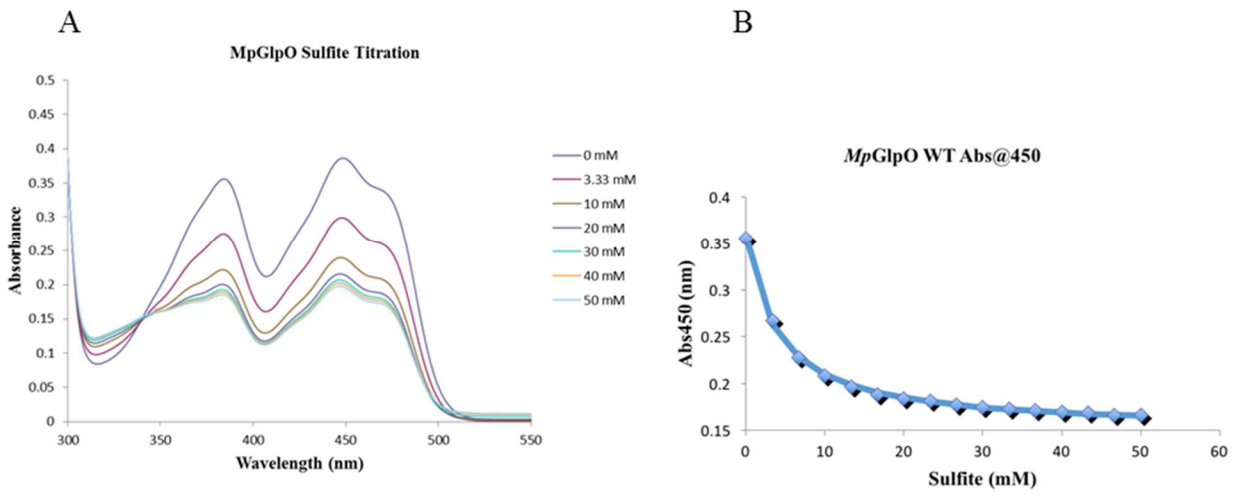

Figure 19: (A) Sulfite titrations of MpGlpO wild-type. 35.4 micromolar of wild-type was titrated aerobically with a 1 M sodium sulfite solution, and flavin reduction was monitored after each addition of sulfite. The spectra shown correspond to the addition of 0 mM (dark blue), 3.33 mM (red), 10 mM (green), 20 mM (purple), 30 mM (light blue), 40 mM (orange) and 50 mM (gray). (B): Abs450 as a function of added sulfite. The line represents the least square fitted behavior for a 1:1 complex formation of enzyme:enzyme-sulfite.

When the H51Q mutant was titrated with sulfite, less than 5% of the enzyme reacted with sulfite (Figure 20) and the calculated K_d for the H51Q mutant was approximately 300 mM. a one hundred-fold increase compared to the wild-type enzyme. We believe that the reduced adduct formation and the increase in the K_d indicates that the histdine residue contributes significantly to the formation of the FMN-sulfite adduct. Elkhal *et al.* proposed that the His51 and Ser348 residues are in a close enough position that allows for efficient adduct formation.[13] These differences are likely due to the absence of favorable interactions with the histidine side chain and steric factors in the mutation with a glutamine.[34] One possible hypothesis that explains why roughly half of the enzyme forms the reversible sulfite adduct is the existence of two species of enzyme during the reaction, one fast-reacting species and one slow-reacting species, which is seen in Table 2. It is possible that the slow-reacting species is unable to form the sulfite adduct. The crystal structure paper on *Mp*GlpO wild-type published by *Elkhal et al*. also witnessed a

50% in absorbance upon titration with sulfite, but they were unable to offer any explanations as to why only half of *Mp*GlpO reacts with sulfite.

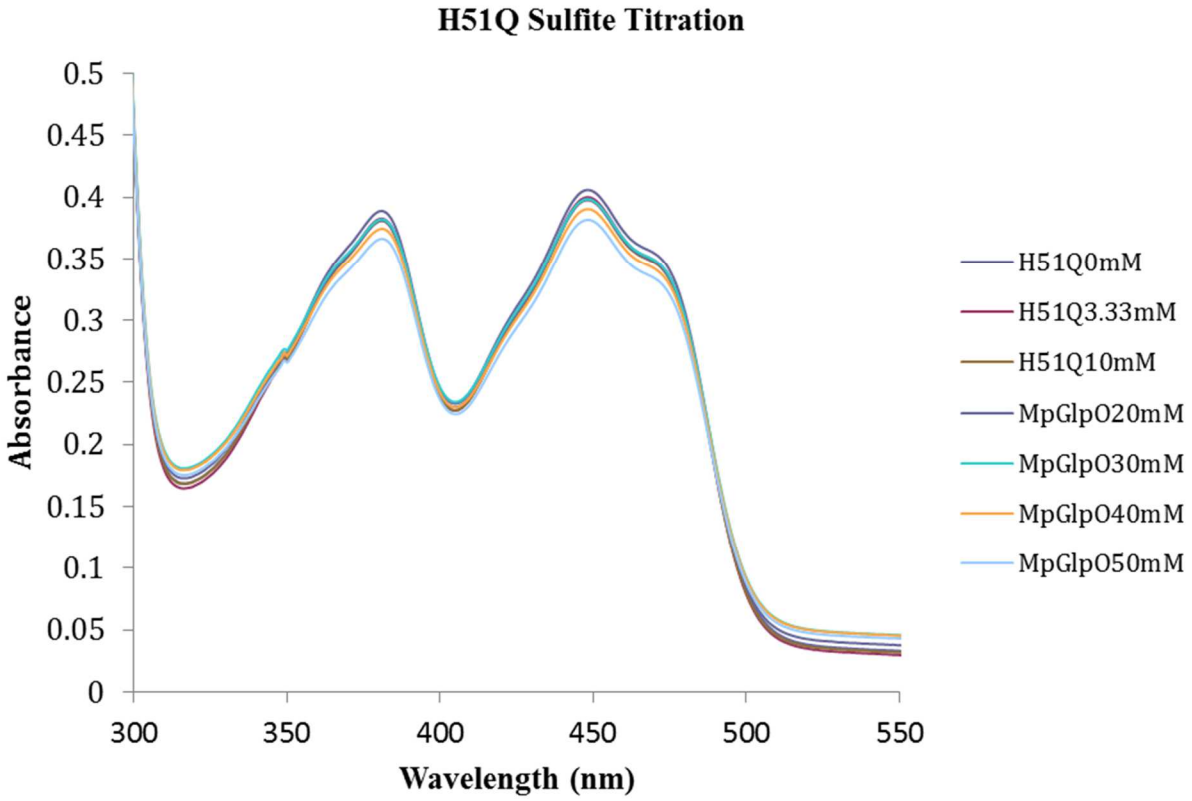

Figure 20: Sulfite titrations of MpGlpO mutant H51Q. 35.4 micromolar of mutant enzyme was titrated aerobically with a 1 M sodium sulfite solution, and flavin reduction was monitored after each addition of sulfite. The spectra shown correspond to the addition of 0 mM (dark blue), 3.33 mM (red), 10 mM (green), 20 mM (purple), 30 mM (light blue), 40 mM (orange) and 50 mM (gray).

Titration of the serine mutant with sulfite (Figure 21) led to behavior like neither the wild-type nor the histidine mutant. The serine mutant becomes fully reduced upon titration with sulfite, whereas only half of the *Mp*GlpO enzyme reacted with sulfite. Plotting the absorbance at 450 nm versus sulfite concentration concluded that the K_d for the S348A mutant was approximately 6 mM, which is two-fold higher than the K_d of wild-type. The slight increase in

K_d of the Ser348 also illustrates that the residue is contributing to the sulfite-adduct formation. These differences in the FMN-sulfite adduct spectra of the S348A mutant indicate that the Ser348 residue plays a role in only half of the FAD being reduced in wild-type enzyme. Because of the close proximity of the Ser348 residue with the flavin, the oxygen atom from Ser348 is 4.6 Å away from the flavin N5-atom, the amino acid could have a role in formation of the sulfite adduct.

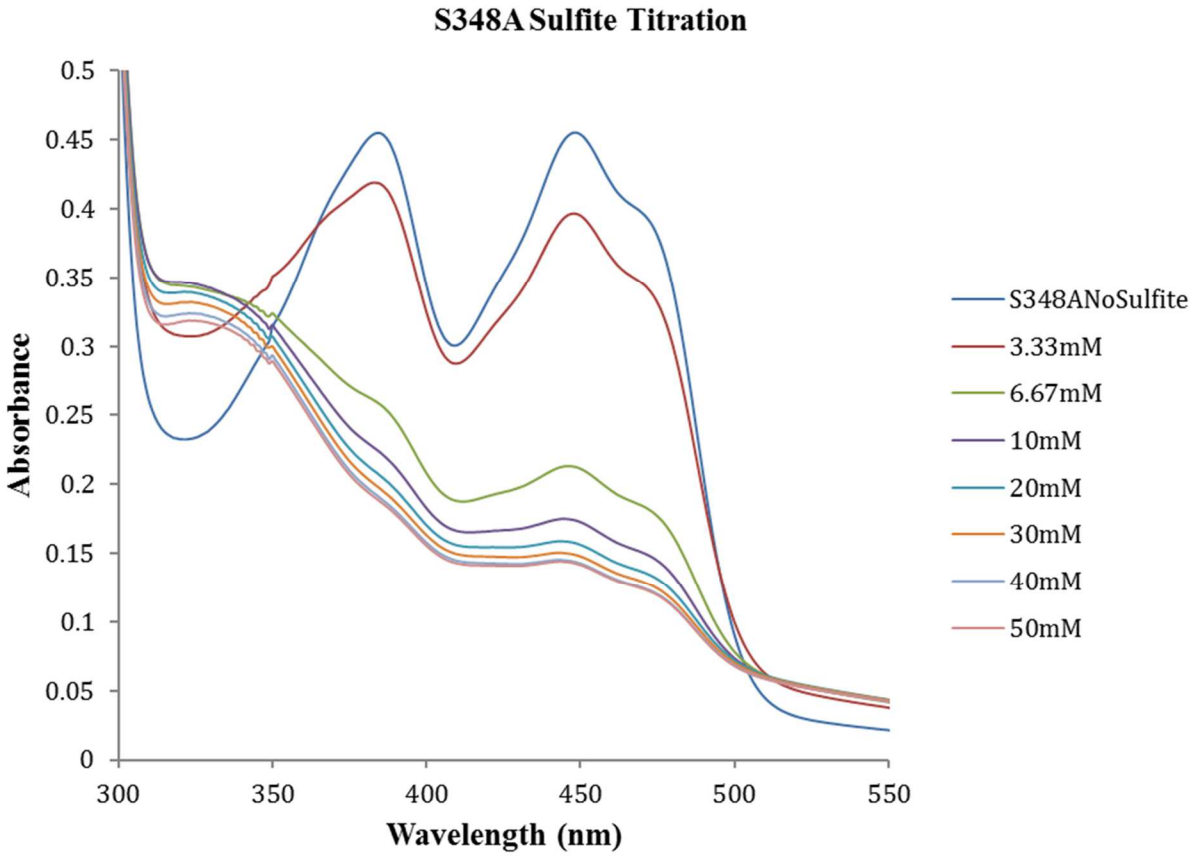

Figure 21: Sulfite titrations of MpGlpO mutant S348A. 35.4 micromolar of mutant enzyme was titrated aerobically with a 1 M sodium sulfite solution, and flavin reduction was monitored after each addition of sulfite. The spectra shown correspond to the addition of 0 mM (dark blue), 3.33 mM (red), 6.67 mM (green), 10 mM (purple), 20 mM (light blue), 30 mM (orange) and 40 mM (gray) and 50 mM (pink).

It is possible that the His51 residue directly contributes to the binding of the sulfite adduct, while the Ser348 residue observed in type II GlpOs while not available in type I, plays an important role in the observed changes in redox potential by affecting the flavin electrostatic environment that impairs the ability of half of the enzyme to bind. *S*spGlpO illustrates full sulfite reduction and does not have the Ser residue available in the active site of the enzyme, instead of the Ser residue *S*spGlpO has a Lys residue in its active site.[4] This change from the positively charged lysine in type I GlpOs to the neutral charged side chain serine in the type II *Mp*GlpO could result in the two varying sulfite-adduct formations of the type I and type II enzymes.

4.5. PH TITRATION USING MULTI-BUFFER SYSTEMS

Attempts at determining the pKa of the important catalytic residues were done using a pH titration. The activity of the *Mp*GlpO wild-type enzyme was analyzed from pH 3 to pH 10 by monitoring the increase in absorbance at 420 nm due to oxidation of the ABTS. A plot of activity vs pH of buffer (Figure 22) illustrates that the wild-type enzyme exhibits different activities at different pH values. This leads us to believe that the protonation state of the histidine in the active site could be important for proper substrate recognition. Because the low pHs tested exhibited little to no activity when compared to pH 7.0 or higher, it leads us to believe that a deprotonated histidine is essential for hydrogen bonding with the substrate. However, attempts at repeating the experiment was unsuccessful as the lower pH buffer solutions failed to hold after the substrate was added to the assay solution. It is unclear why the buffer held at the proper pH the first time and unable to hold on following attempts. The first attempt at the pH titration illustrates that the pK_a of the active site in *Mp*GlpO is between 6 and 8, and we would

expect that value to correspond with perhaps histidine which has a side chain pK_a of 6.04 and a pI of 7.58.

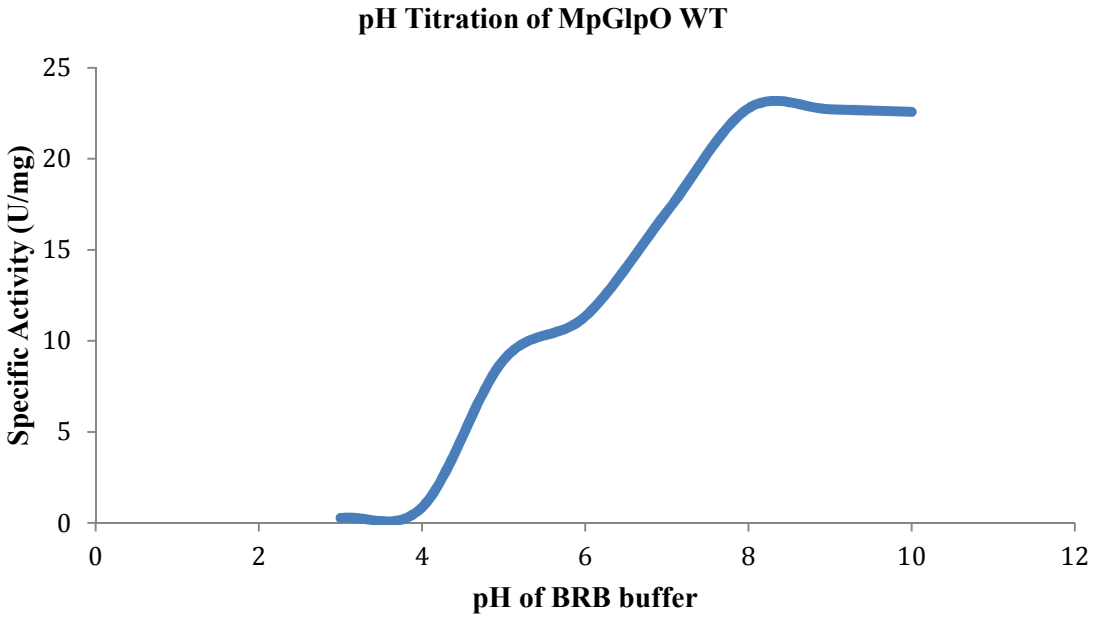

Figure 22: pH titration of *Mp*GlpO wild-type enzyme using Britton Robinson Buffer, at 25 ºC, at various pHs to test specific activity. Specific activity was determined by monitoring the reaction at 420 nm using the ABTS-HRP coupled assay previously described.

If a buffer-system that holds at low pHs upon addition of the glycerophosphate substrate could be found, a pH titration of the wild-type enzyme would be useful in determining the pK_a of the active site of *Mp*GlpO.

4.6. EXPRESSION OF *S*SPGLPO

Sufficient growth was seen following a protocol suggested by Dr. Derek Parsonage (Wake Forest University) in each of the tested media, but after running a SDS-PAGE gel on samples before and after induction, there was no evidence of production of the correct protein. Attempts at purification of *S*spGlpO wild-type enzyme were also performed, resulting in SDS-

PAGE gels with multiple bands appearing in the pooled fractions, instead of one band at the correct size, illustrating a potential proteolysis (Figure 23).

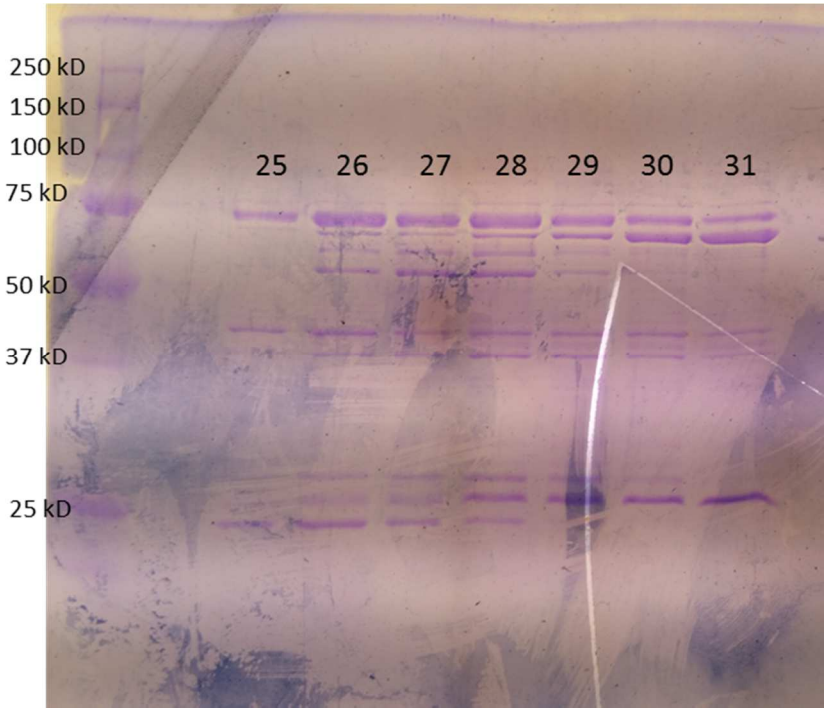

Figure 23: SDS-PAGE gel of *S*spGlpO protein fractions after Q column (cation exchange). The ladder used is Precision Plus Protein Standards and are listed to the left of the corresponding band in the figure. The fraction number is labeled above the corresponding lane.

Previous studies have shown that the H65Q mutation in *S*spGlpO retains 63% of wild-type activity, unlike the H51Q mutation in *Mp*GlpO which results in approximately 7% of wild-type activity. However, the data involving *S*spGlpO His65 mutations was acquired from a well plate and need the experiments need to be performed using a different instrument to verify the results. It is important to note that the same substitution in the two enzymes result in vastly different activities and understanding the differences between the type I and type II enzymes will be useful in figuring out why this happens. The H65Q mutation in *S*spGlpO retained approximately 63% of wild-type activity while the H65A mutation only had 2% of activity

remaining. Although the H51A mutation only had 1.3% of wild-type activity, comparable to the 2% of wild-type activity of H65A in *S*spGlpO. It could be possible that in *S*spGlpO there is a nearby residue that can assist the glutamine residue in establishing catalytic activity when the histidine is mutated into a glutamine, however when the histidine is mutated into an alanine then almost no activity is seen. One possibility that explains these results is that the polar charge that is seen in both histidine and glutamine, but not alanine, is necessary for efficient catalytic activity. It is also possible that the residues must be able to act as hydrogen bond donors in order to establish catalytic activity, or that the mutations of the residues are no longer sterically ideal to be able to interact with the glycerophosphate substrate.

CHAPTER 5. CONCLUSIONS AND FUTURE WORK

In conclusion, we have confirmed that His51 is important in hydrogen bonding to the Glp substrate. Based on the model shown in Figure 9, His51 could function as a hydrogen bond donor or acceptor from the C2 of Glp. It could be possible that a water molecule is acting as the base in the reaction, with the His51 residue being essential for recognition of the substrate. Using the specific activity determined from the ABTS-HRP coupled assay we have concluded that mutation of this residue to a glutamine or an alanine results in compromised activity when compared to wild-type, illustrating its important role in the catalytic activity of the *Mp*GlpO enzyme. Mutations of the Ser348 residue with an alanine also results in severely reduced activity of the *Mp*GlpO enzyme providing strong support for the model of Glp binding presented in Figure 9. This work suggests that the Ser 348 residue influences the redox potential of the flavin, as mutations of this amino acid causes the flavin to become completely reduced during sulfite titrations. Future work in this area will focus on determining the Flavin redox potential in the mutants. Apparent steady-state kinetics at 25 ^{o}C and pH 7.0 revealed that the wild-type enzyme has a K_m^{Glp} of 14 mM and a K_{cat} of 75 s^{-1}, resulting in a specificity constant of 5.3 $mM^{-1}*s^{-1}$. The specific activity of the wild-type enzyme and H51Q, H51A, and S348A mutants were determined to be 34.7 $U*mg^{-1}$, 2.22 $U*mg^{-1}$, 0.45 $U*mg^{-1}$, and 0.62 $U*mg^{-1}$, respectively. The fact that H51Q has slightly more activity than H51A leads to the conclusion that a polar side chain is necessary for efficient conversion of substrate to product through the use of hydrogen bonding with the polar residue. The data demonstrates that the His side chain is important, as a simple substitution to another polar side chain does not restore wild-type activity levels. Sulfite titrations also revealed the importance of His51 in the ability of *Mp*GlpO to form the sulfite-

adduct, and a completely different sulfite profile than wild-type when the Ser348 residue is mutated. It is likely that mutations of the Ser348 residue causes a change in the redox potential between the type I and type II GlpOs. In the S348A mutant the flavin becomes fully reduced upon titration with sulfite, revealing that in this mutant the flavin more readily receives electrons. It is also likely that the H51Q mutation causes the enzyme to no longer be able to efficiently bind to sulfite and the His residue is necessary for sulfite-adduct formation.

Future work to be done with the *Mp*GlpO enzyme will be to complete the mutations for the rest of the amino acids located in the active site that are predicted to bind the substrate. In particular we are interested in mutating R320, K258, F250, S47, and Y234, which are shown in Figure 6. Mutant K258M has already been harvested following the established protocol. The R320M mutant was not obtained, to date, and requires resequencing. The K258M mutant has been sequenced and expressed and is ready for protein purification. It could also be of interest to perform a double mutation, a H51AS348A mutation of both critical residues in the active site to see if the resulting enzyme, assuming it would be properly folded, would retain any wild-type activity.

Using the predicted binding model from Elkhal *et al*., the roles of the amino acids in the active site of the enzyme are able to be predicted based on their location and composition of the residue (Figure 10A). Arg320 is predicted to be involved in electrostatic/hydrogen-bonding interactions with the phosphoryl group on the Glp substrate. Arg320 is conserved in all 72 close relatives of *Mp*GlpO. Lys258 is also conserved in all 72 relatives of *Mp*GlpO and is predicted to interact with the phosphoryl group on Glp. Phe250 is conserved in all 72 *Mp*GlpO relatives and is predicted to help stabilize the C_1 hydroxymethyl group on the glycerol domain of glycerophosphate. Ser47 is predicted to interact with both a hydroxyl on Tyr234 as well as the

flavin cofactor. Ser47 is conserved in 70 *Mp*GlpO relatives and replaced, conservatively by Thr in two. Mutating the Ser47 residue with an alanine would disrupt the interactions with the Tyr234 hydroxyl and FAD. The Tyr234 mutation would test the importance of its interaction with Ser47. The Ser47 hydroxyl, supported by its interactions with Tyr234, is well placed to help stabilize the protonated N5 of the reduced flavin.[13] This could provide further insight into the catalytic mechanism of *Mp*GlpO and help illustrate the differences between the type I and type II GlpOs. Out of the previously mentioned residues, R320 is conserved in type I and type II GlpOs, while Ph3250, Ser47 & Tyr234 are replaced by similar residues in type I GlpOs, and there is no Lys258 equivalent in *S*spGlpO (Figure 6C). It would also be of interest to obtain the crystal structure of the wild-type *Mp*GlpO enzyme with the glycerophosphate substrate bound in an attempt to validate the binding mechanism. Acquiring a stopped-flow instrument to perform enzyme-monitored turnover experiments in order to understand the rate-limiting steps of my mutants. This will be accomplished by monitoring the reductive and oxidative half-reactions to see where the mutants are impacting the activity of the enzyme.

It would likewise be of interest to pursue attempts at chemical rescue of the H51A mutant using imidazole. Illustrating that the addition of imidazole, which has a structure closely related to a histidine side chain, rescues the activity of the enzyme would further prove the importance of the histidine side chain in the activity of *Mp*GlpO wild-type. The H51A mutant protein activity was measured in the same conditions as the standard assay with varying concentrations of imidazole. Imidazole concentrations were varied from 0 to 100 mM and were added to the assay mixture from concentrated stocks adjusted to pH 7.0. However, the imidazole rescue resulted in being unable to obtain any measurable change in the rate of the enzyme with varying

concentrations of imidazole. Further study in order to determine if rescue of activity is achievable using a higher concentration of enzyme than previously attempted.

Another topic that could be of interest as a future goal would be to continue to try to determine the pK_a of the active site of *Mp*GlpO using pH titrations. Revealing the pK_a of the active site could shed some light on the residues in the active site that could be assisting His 51 in acting as the catalytic base in the *Mp*GlpO reaction. Finding a multi-buffer system that holds at low pHs when the glycerophosphate is added is necessary for determining the pK_a of the active site of *Mp*GlpO. One caveat however, is that there is a possibility of the protein becoming misfolded at the low pH regions. In order to verify that the enzyme has not altered its folding pattern would be to look at the fingerprint region of the flavin using Infrared spectroscopy before and after varying the pH values. It could also be possible to make sure the protein keeps its folding pattern at low pH values using circular dichroism spectroscopy to see if the percentage of alpha-helices and beta-sheets differs upon changing the pH.

The last future goal for this study would be to establish a protocol to obtain successful expression of *S*spGlpO in order to verify the results obtained from our collaborators. If the type I GlpO *S*spGlpO truly retains 63% of wild-type activity, it would be likely that the two types of GlpOs utilize different catalytic mechanisms. If type I and type II GlpOs utilize different mechanisms it could be possible to develop small molecule inhibitors against *Mp*GlpO for future drug development against *Mycoplasma pneumoniae* infections.

CHAPTER 6. WORKS CITED

(1) Fagan, R.L. & Palfey, B.A. (2010) Flavin-dependent enzymes. In *Comprehensive Natural Products II Chemistry and Biology* (Vol. 7) (Mander, L. and Liu, H-w., eds) Elsevier Science, 37-113

(2) Silverman, Richard B. (1992) "Flavin." *The Organic Chemistry of Drug Design and Drug Action*. San Diego: Academic, 132-137.

(3) Kim HJ, Winge DR (May 2013). "Emerging concepts in the flavinylation of succinate dehydrogenase". Biochimica et Biophysica Acta **1827** (5): 627–36.

(4) Chaiyen, P.; Fraaije, M.W. & Mattevi, A. (2012) The enigmatic reaction of flavins with oxygen. *Trends Biochem Sci* **37**, 373–380.

(5) Lennicke, C.; Rahn, J.; Lichtenfels, R.; Wessjohann, L.A. & Seliger B (2015) Hydrogen peroxide – production, fate and role in redox signaling of tumor cells. *Cell Communication and Signaling* **13**:39

(6) Marinho, H.S.; Real, C.; Cyrne, L.; Soares, H. & Antunes, F. (2014) Hydrogen peroxide sensing, signaling and regulation of transcription factors. *Redox Biology* **2**, 535-562

(7) Makarov, V. et al. (2009) Benzothiazinones kill *Mycoplasma tuberculosis* by blocking arabinan synthesis. *Science* **324**, 801-804

(8) Macdonald, M.J. & Brown, L. J. (1996) Calcium activation of mitochondrial glycerol phosphate dehydrogenase restudied, *Arch. Biochem. Biophys.* ***326,*** 79-84.

(9) Austin, D. & Larson, T. J. (1991) Nucleotide sequence of the *glpD* gene encoding aerobic *sn*-glycerol 3-phosphate dehydrogenase of *Escherichia coli* K-12, J. *Bacteriol.* ***173,*** 101-107.

(10) Colussi, T.; Parsonage, D.; Boles, W.; Matsuoka, T.; Mallett, TC.; Karp lus, P.A. & Claiborne, A. (2008) Structure of alpha-glycerophosphate oxidase from *Streptococcus sp*.: a template for the mitochondrial alpha-glycerophosphate dehydrogenase. *Biochemistry* **47**, 965–977.

(11) Esders, T. W. & Michrina, C. A. (1979) Purification and properties of L-alpha-glycerophosphate from *Streptococcus faecium* ATCC 12755, *J. Biol. Chem.* ***254,*** 2710-2715

(12) Claiborne, A. (1986) Studies on the structure and mechanism of *Streptococcus faecium* L-alpha glycerophosphate oxidase, *J. Biol. Chem.* ***261,*** *14398-14407*

(13) Elkhal, CK.; Kean, K.; Parsonage, D.; Maenpuen, S.; Chaiyen, P.; Claiborne, A. & Karplus P.A. (2015) Structure and proposed mechanism of a-glycerophosphate oxidase from *Mycoplasma pneumoniae*. FEBS J **282**, 3030-3042

(14) Parsonage, D.; Luba, J.; Mallett, T. C.; & Claiborne, A. (1998) The soluble R-glycerophosphate oxidase from *Enterococcus casseliflavus*. Sequence homology with the membrane-associated dehydrogenase and kinetic analysis of the recombinant enzyme, *J. Biol. Chem.* ***273***, 23812-23822.

(15) Charrier, V.; Luba, J.; Parsonage, D. & Claiborne, A. (2000) Limited proteolysis as a structural probe of the soluble alpha-glycerophosphate oxidase from *Streptococcus* sp. *Biochemistry* **39**, 5035–5044.

(16) Maenpuen, S.; Watthaisong, P.; Supon, P.; Sucharitakul, J.; Parsonage, D.; Karplus, P.A.; Claiborne, A. & Chaiyen, P. (2015) Kinetic mechanism of L-a-glycerophosphate oxidase from mycoplasma pneumoniae. FEBS J. **282**, 3043-3059

(17) Pilo, P.; Vilei, EM.; Peterhans, E.; Bonvin-Klotz, L.; Stoffel, MH.; Dobbelaere, D. & Frey, J. (2005) A metabolic enzyme as a primary virulence factor of *Mycoplasma mycoides* subsp. mycoides small colony. *J Bacteriol* **187**, 6824–6831.

(18) Yeh, J. I.; Du, S.; Tortajada, A.; Paulo, J. & Zhang, S. (2005) Peptergents: Peptide detergents that improve stability and functionality of a membrane protein, glycerol-3-phosphate dehydrogenase, *Biochemistry* ***44,*** 16912-16919

(19) Hedin, T. (1991) Glycerol-3-phosphate dehydrogenase of *Bacillus subtilis* BR95: Cellular localization, biochemical properties and reconstitution into natural and artificial membranes, Master's thesis, University of Lund, Lund, Sweden.

(20) Fairlamb, A.H. & Bowman, I.B.R. (1977) Inhibitor studies on particulate *sn*-glycerol-3-phosphate oxidase from *Trypanosoma brucei*. *Int J Biochem* **8**, 669-675.

(21) Waites, K.B. & Talkington, D.F. (2004) *Mycoplasma pneumoniae* and its role as a human pathogen. *Clin Microbiol* Rev **17**, 697–728.

(22) Hames, C.; Halbedel, S.; Hoppert, M.; Frey, J. & Stulke, J. (2009) Glycerol metabolism is important for cytotoxicity of *Mycoplasma pneumoniae*. J Bacteriol **191**, 747–753.

(23) Madhi, L.K.; Wang, H.; Van der Hoek, M.B.; Paton, J.C. & Ogunniyi, A.D. (2012) Identification of a novel pneumococcal vaccine antigen preferentially expressed during meningitis in mice. *J Clin Invest* **122**, 2208-2220.

(24) Finnerty, C. M.; Charrier, V.; Claiborne, A.; & Karplus, P. A. (2002) Crystallization and preliminary crystallographic analysis of the soluble R-glycerophosphate oxidase from *Streptococcus* sp., *Acta Crystallogr. D58*, 165-166.

(25) *StrataClone PCR Cloning Kit*. *Stratagene Manual*. Web. http://www.agilent.com/cs/library/usermanuals/Public/240205.pdf

(26) Pitsawong, W.; Sucharitakul, J.; Prongjit, M.; Tan, TC.; Spadiut, O.; Haltrich, D.; Divne, C. & Chaiyen, P. (2010) A conserved active-site threonine is important for both sugar and flavin oxidations of pyranose 2-oxidase. *J Biol Chem* **285**, 9697-9705

(27) Massey, V.; Muller, F.; Feldberg, R.; Schuman, M.; Sullivan, P.A.; Howell, L.G.; Mayhew, S.G.; Matthews, R.G. & Foust, G.P. (1969) The reactivity of flavoproteins with sulfite: possible relevance to the problem of oxygen reactivity. *J Biol Chem* **244**, 3999–4006.

(28) Berg, J.M.; Tymoczko, J.L. & Stryer, L. Biochemistry. 5th edition. New York: W H Freeman; 2002. Section 8.4, The Michaelis-Menten Model Accounts for the Kinetic Properties of Many Enzymes.

(29) Ebihara, A.; Kawamoto, S.; Shibata, N.; Yamaguchi, T.; Suzuki, F.; Nakagawa, T. (2016) Development of a modified Britton-Robinson buffer with improved linearity in the alkaline pH region. *Biojournal of Science and Technology*. **3**, 2016

(30) Nelson, K.J.; Day, A.E.; Zeng, B.; King, S.B.,; & Poole, L.B. (2008) Isotope-coded, iodoacetamide-based reagent to determine individual cysteine pK_a values by matrix-assisted laser desorption/ionization time-of-flight mass spectrometry. *Analytical Biochemistry* **375**, 187-195

(31) Argueta, E.A.; Amoh, A.N.; Kafle, P. & Schneider, T.L. (2015) Unusual non-enzymatic flavin catalysis enhances understanding of flavoenzymes. *FEBS Letters.* **589**, 880-884

(32) Taylor WR. (1986) The classification of amino acid conservation. *J Theor Bio* **119**, 205-218

(33) Tegoni, M. & Matthews, F.S. (1988) Crystallographic study of the complex beteen sulfite and baker's yeast flavocytochrome b_2 *J. Biol. Chem.* **263**, 19278-19281

(34) Lehoux, I.E. & Mitra, B. (1999) (S)-Mandelate Dehydrogenase from *Pseudomonas putida*: Mutations of the Catalytic Base Histidine-274 and Chemical Rescue of Activity *Biochemistry,* **38,** 9948-9955